Genetic analysis and transcriptome profile characterizing pathogenesis of host response to Sendai virus infection in mice

by

Ayo Yila, SIMON
D. V. M (Ahmadu Bello University, Zaria) 1991
M. Sc (Ahmadu Bello University, Zaria) 2002

A dissertation submitted to the Graduate School of Veterinary Medicine, Hokkaido University in partial fulfillment of the requirements for the degree of Doctor of Philosophy (PhD)

Laboratory of Laboratory Animal Science and Medicine
Department of Disease Control
Graduate School of Veterinary Medicine
Hokkaido University Sapporo, JAPAN

February, 2010

DEDICATION

To my beloved wife Dr Mrs. Thamar A Yila and daughter Zarah Yila Simon for giving me new dreams to pursue

ACKNOWLEDGEMENTS

First of all I would like to reverence and thank the Lord God Almighty for his constant blessings and guidance through out the course of this study. I would also like to specially thank my supervisor Professor Takashi Agui for welcoming me to his Laboratory, for sharing his knowledge and for his encouragement which helped during my work. A personal and big thank you to Associate Professors Nobuya Sasaki and Atushi Asano, who were always there since the beginning and who helped me become a better scientist (and a better person too...) I express my gratitude to Professor Yasuhiro Kon and Assistant Professor Osamu Ichii for their valuable contribution towards achieving the objectives of this research. I wish to extend my gratitude to Professor Kazuhiko Ohashi and Associate Professor Satoru Konnai for accepting to be the examiners of the thesis jury. I also thank all the former and current members of the lab for their support and encouragement during the period of my PhD work. Last but not least, I would like to thank my family and friends for their encouragement and support during the course of my studies and for making my stay in Sapporo, something to always remember.

Preface

Respiratory paramyxoviral infections are leading cause of serious respiratory disease in humans especially among children. Murine models of viral respiratory disease have many similar traits to human respiratory infections and can be use to investigate the mechanism of susceptibility associated with disease severity. Sendai virus (SeV) is thought to be the natural rodent pathogen; however, it has been shown to infect sub-human primate experimentally, which could theoretically infect humans. In addition, studies in inbred mice had revealed a wide spectrum of resistance and susceptibility to SeV. Thus, suggesting that genetic factors could be playing a crucial role in natural resistance to these closely related viruses. Earlier reports based on genetic differences generated an array of hypotheses about associated phenotypic characteristic (sex and coat colour) or underlying gene polymorphisms such as Interferon (IFN), mucocilliary transport or Sas-1, toll-like receptors (TLR), and H-2 haplotype, none of which fully confirmed the genetic basis of the varying spectrum of resistance and susceptibility to SeV. Since resistance and susceptibility to infection are complex genetic traits, and as a step towards the elucidation of the contributing genetic host factors responsible for the differences to SeV infection in mice, the first aspect of the study involves carrying out genetic mapping studies in DBA/2 (D2) (susceptible) and C57BL/6 (B6) (resistant) mice with the goal of dissecting the genetic variants, which might provide valuable insights into the molecular basis of host variations to SeV infection.

Furthermore, the severity of respiratory viral infections in humans varies in clinical presentations and pathological outcomes. SeV is known to display a wide spectrum of resistance and susceptibility among mice strains. However, the variation in sensitivity to SeV was not only because of genetic restriction of viral infection and replication rather was the result of some aberrations or differences in the

humoral or cell-mediated immune response. In addition, evidence has been accumulating that children with severe respiratory infection suffer from enhanced inflammatory lesions cause by cytokine storm, rather than virus induced cytopathology. To define the beneficial or detrimental pulmonary immune response to SeV infection in mice, the author further characterized the transcriptome profile of the pathogenesis of SeV infection in these two mice strains, by analyzing cellular infiltrations, histopathology, bronchoalveolar lavage fluid cytokines as well as inflammatory gene expression profile using a novel cDNA reverse transcriptase–polymerase chain reaction array (RT-PCRarray) prepared from the lungs of B6 and D2 infected mice on days 2, 4, 8 and 14.

Abbreviations

B6	C57BL/6J
BALF	Bronchoalveolar lavage fluid
C	Cysteine
CC	Cysteine-cysteine-chemokines (β-chemokine)
Chr	Chromosome
cM	CentiMorgans
CXC	Cysteine -X- cysteine-chemokines (α-chemokines)
D2	DBA/2J
DMEM	Dulbecco's modified Eagle Medium
EDTA	Ethylenediaminetetraacetic acid
F	Fusion protein
FBS	Fetal bovine serum
G	Guanine
h	Hour
HBSS	Hank's balanced Salt Solution
HN	Hemagglutinin neuraminidase
HPIVI	Human parainfluenza virus type 1
IFN	Interferon
IL	Interleukin
Kb	Kilobase
L	Large protein
LOD	Likelihood of the Odds
LRS	Likelihood ratio statistic
M	Matrix protein
Mb	Megabase
MDA5	Melanoma differentiation-associated gene 5
MeV	Measles virus

min	Minutes
MV	Mumps virus
NC	Nucleocapsid
NNV	Nonsegmented negative stranded RNA virus
NP	Nucleoprotein
ORF	Open reading frame
P	Phosphoprotein
PBS	Phosphate-buffered saline
PCR	Polymerase chain reaction
p.i	Post infection
QTL	Quantitative trait locus
QT	Quantitative trait
RANTES	Regulated upon activation, normal T cell expressed and secreted
RIG-1	Retinoic-acid-inducible gene I
RSV	Respiratory syncytial virus
RT-PCR	Reverse transcriptase-polymerase chain reaction
s	Seconds
SARS	Severe acute respiratory syndrome
SDS	Sodium dodecyl sulfate
SE	Standard error
SeV	Sendai virus
TCID50	50% tissue infectious dose
TNF	Tumour Necrosis Factor
Tlr	Toll-like receptor
Th_1	Type 1 helper T cells
Th_2	Type 2 helper T cells
U	Uracil
vRNAP	Viral RNA polymerase

VSV	Vesicular stomatitis virus

TABLE OF CONTENTS

1.0 General Introduction

Sendai virus (SeV) was discovered in Japan in 1953. It was isolated in the Tohoku University Hospital from a newborn patient presenting pneumonia syndromes. SeV is also referred to as murine parainfluenza type I virus as it was found to infect respiratory tract of mice and causes pneumonia which spreads to uninfected animals. SeV is currently an important respiratory pathogen of laboratory rodents, causing epidemics with high mortality during the acute phase. It is extremely contagious and transmission occurs via contact and aerosol infection of the respiratory tract. SeV is an enveloped non-segmented negative stranded RNA virus (NNV) of the *Paramyxoviridae* family, subfamily *Paramyxovirinae* and genus Paramyxovirus (or Respirovirus). The scientific community also considers SeV as the archetype organism of the *Paramyxoviridae* family because most of the basic biochemical, molecular and biologic properties of the whole family were derived from its own characteristics. Therefore, it is considered to be a good model for the study of the *Paramyxoviridae* family because it includes significant human pathogens of infants and children, such as Mumps virus (MV), Measles virus (MeV), Respiratory syncytial virus (RSV) and Nipah virus (Chanock, 2001). Some of these viruses are still importantly prevalent in developing countries (e.g. MeV still causes million deaths/year) and with others which have only recently emerged. Thus, studies on SeV can offer important information for understanding of the molecular mechanisms of this virus family and consequently offer better treatment and control strategies.

The *Paramyxoviridae* family along with the *Rhabdoviridae*, the *Filoviridae* and the *Bornaviridae* families, are all part of the *Mononegalvirales* order. It is subdivided into two subfamilies:

the *Paramyxovirinae* containing the *Respiro*-, the *Rubula*-, the *Morbilli*-, the *Avula*- and the *Henipa*-viruses; and the *Pneumovirinae*, containing the *Pneumo*- and the *Metapneumo*-viruses. Emergence of new paramyxoviruses, such as Hendra and Nipah, causing respiratory and neurological disease in pigs and humans, has been observed recently. The classification of these different viruses is based on morphologic criteria, the organization of the genome, the biological activities of the proteins, and the sequence relationship of the encoded proteins (Table 1.1). The Mononegalviruses share a number of fundamental characteristics: (1) Their genome is a single negative stranded RNA, packaged in a helical nucleocapsid (NC); (2) nucleocapsids are enclosed within an envelope derived from the plasma membrane of the cell; (3) a virus-coded RNA polymerase packaged in the virion synthesizes the viral mRNAs by transcribing the RNA as part of the intact NC after it enters the cell; (4) the RNA polymerase begins transcribing at the 3'end of the genome RNA and sequentially transcribes 5-10 genes, terminating and releasing each mRNA before starting the next one.

Table 1.1: Classification of the *Paramyxoviridae* family

Classification of the *Paramyxoviridae* family
Family *Paramyxoviridae*
Subfamily *Paramyxovirinae*
Genus Respirovirus (Paramyxovirus)
Sendai virus (mouse parainfluenza virus type 1)
Human parainfluenza virus type 1 and 3
Bovine parainfluenza virus type 3
Simian virus 10
Genus Rubulavirus
Simian virus 5 (Canine parainfluenza virus type 5)
Mumps virus
Human parainfluenza virus type 2, type 4a and 4b
Porcine rubulavirus
Genus Morbillivirus
Measles virus
Dolphin morbillivirus
Canine distemper virus
Peste-des-petits-ruminants virus
Phocine distemper virus
Rinderpest virus
Cetacean morbillivirus
Genus Avulavirus
Newcastle disease virus (avian paramyxovirus 1)
Genus Henipavirus
Hendra virus
Nipah virus
Subfamily *Pneumovirinae*
Genus Pneumovirus
Human respiratory syncytial virus
Bovine respiratory syncytial virus
Murine pneumonia virus (Pneumonia virus of mice)
Genus Metapneumovirus
Avian pneumovirus
Unclassified paramyxoviruses
Tupaia Paramyxovirus

1.1. Virion structure of Sendai virus

Sendai virus particles are pleomorphic structures composed of a lipoprotein envelope surrounding a single unsegmented viral nucleocapsid. The viral envelope is composed of a lipid bilayer containing the viral fusion (F) protein, the hemagglutinin/neuraminidase (HN) protein, and the matrix (M) protein which forms an electron-dense shell immediately below the membrane (Le Mercier et al., 2003). The F glycoprotein mediates fusion of the viral envelope with the cellular membrane and also assists in viral attachment. In addition it mediates cell–cell fusion leading to the formation of a syncytium and extension of infection in the local area (Sanderson et al., 1993).

To acquire biological activity the F glycoprotein must be cleaved by a cellular protease into two disulfide-linked polypeptides, F1 and F2. When a host cell does not contain appropriate proteases, the virus formed is not infectious (Blumberg et al., 1985). The HN glycoprotein mediates the first step in viral infection, and viral adsorption by attachment to cellular surface receptors. Late in infection the HN also causes enzymatic cleavage of sialic acid (neuraminic acid) residues on the virus that must be removed to prevent self-aggregation of virus particles during release from infected cells (Chanock, 2001). The M protein is considered to play a central role in virion formation. SeV virions are formed in so-called lipid rafts on the cell membrane (Ali and Nayak, 2000). At these sites, M protein is thought to enhance virion formation by concentrating the spike proteins and the viral ribonucleoproteins. It has been demonstrated that M protein indeed binds to the cytoplasmatic tail of the spike proteins and to the ribonucleoproteins (Sanderson et al., 1993; Coronel et al., 2001). Thus, M protein has the capacity to mediate the binding of many of these viral components to lipids. In addition, it has been found that overexpression of the M proteins causes the budding of virus-like particles (Takimoto et al., 2001).

These findings indicate that M protein functions as a driving force for virus assembly and budding.

1.2. Genome organization and encoded proteins

The SeV genome is a single stranded negative sense RNA, 15–16 kb in length (Chanock, 2001). Like other parainfluenza viruses, the genome is organized starting with a short 30-leader region, followed by 5–10 genes, and ending with the short 50-trailer region. The SeV genome encodes the six structural proteins: the two surface glycoproteins HN and F; three nucleocapsid proteins N, P, and L, and the non-glycosylated internal protein M, the order of which is 3′ – (leader) – NP-P-M-F-HN-L-(trailer)- 5′ (Blanchard et al., 2004; Lamb and Kolakofsky, 2001)

Coiled around the inside surface of the viral envelope is the nucleocapsid, characterized by large, helical, highly flexible ribonucleoprotein particles, approximately 15 nm in diameter and 1μm in length. It contains the viral genome and three different viral proteins: the nucleoprotein (N), the phospho-protein (P), and the large protein (L) (Lamb and Kolakfsky, 2001). The NP is the major structural component of the nucleocapsid (58 kD), of which 2,600 molecules tightly encapsidate the RNA. Encapsidation renders the RNA inaccessible to RNases and is required for it to serve as a template for the viral RNA-dependent RNA polymerase complex. NP protein plays thus a central role in SeV replication and may be regarded as a regulatory factor that switches the polymerase from the transcriptive to the replicative mode. The two other proteins necessary for polymerase functions are the L protein (251 kDa), which is considered the core of the polymerase complex, and the P protein (65 kDa). Both of these proteins are present in only minor amounts in nucleocapsids. The SeV L protein is the candidate of choice for several multiple enzymatic functions exerted by the nucleocapsid complex, such as initiation, elongation, termination of transcriptional and replicational products as well as methylation,

capping, and polyadenylation of transcripts (Morgan and Rakestraw, 1986; Shioda et al., 1986). The P protein is involved in multiple proteins – protein interactions that are required for RNA synthesis. It complexes with protein L to form the RNA polymerase, appears to be important for the proper folding of the L protein, and also mediates binding of the polymerase to the nucleocapsid (Bowman et al., 1999)

The P and L proteins form the core of the viral RNA dependent RNA polymerase (vRNAP). The vRNAP is involved in the transcription and the replication, which are two important steps in the life-cycle of the virus. For transcription, the polymerase complex is constituted only by the P and L proteins, but for efficient replication, the N protein is required in addition to the L and P proteins. Several studies indicate that there are two different possible states (multiprotein complex) of the polymerase depending on whether it is transcribing or replicating. For example, it has been recently shown that the polymerase of vesicular stomatitis virus (VSV) founds itself in a replicase or in a transcriptase state, depending on its protein composition (Qanungo et al., 2004). There is, however, no indication that this could be the case for the Paramyxovirus RNA polymerase. The polymerase cofactor P protein of SeV forms a tetramer and is named for its highly phosphorylated nature. It is a modular protein with distinct functional domains and is composed of N-terminal and a C-terminal domain separated by hyper variable hinge (Curran and Kolakofsky, 1990). The N-terminal part is a chaperone for unassembled N proteins (N°), preventing it from binding to nonviral RNA in the infected cell (Curran et al., 1995) and forming a complex (P-N°) whose intracellular concentration is believed to regulate rates of transcription and replication from genomic template (Curran et al., 1995; Masters and Banerjee, 1988). The C-terminal part is only functional as an oligomer and forms, along with L, the polymerase complex. It has already been shown for some other paramyxoviruses that the association of the N and P proteins

has an effect on the N conformation (MeV) and on the virus assembly (VSV) (Kingston et al., 2004; Das and Pattnaik, 2005).

The L protein is the largest and the least abundant protein of the structural proteins. Its gene is also the most promoter-distal in the transcriptional map. It binds to the N: RNA template via the P protein and contains all vRNAP catalytic activities like synthesis, capping/polyadenylation and methylation of the nascent viral mRNA (Ogino et al., 2005). The L protein is highly unstable when expressed alone and needs to bind P to confer a good stability and a proper conformation, as co-expression of P and L is necessary for the formation of an active polymerase complex (Curran et al., 1995; Horikami et al., 1997). Until today, no crystal structure of the mononegalvirales L proteins is available. However, primary structure conservation among the RNA polymerases suggests similar protein architecture. Sequence comparisons of NNV-L proteins have identified 6 conserved regions, interrupted by variable sequences. These regions have been proposed to correspond to functional domains of the protein (Poch et al., 1990; Sidhu et al., 1993). There is also new evidence that the L protein could directly interact with itself and that this interaction would help RNA synthesis (Smallwood and Moyer, 2004).

The M protein is the most abundant protein in SeV virion. It is a quite basic and hydrophobic protein. The M protein is considered to be the central organizer in paramyxovirus budding and virus morphogenesis (Sakaguchi et al., 1994b; Mottet et al., 1996). The M protein self-associates and interacts with membranes, forming patches at the inner surface of the plasma membrane (Stricker et al., 1994). It also interacts with the cytoplasmic tails of integral membrane proteins such as the F and HN proteins, the lipid bilayer and the NC (Ali and Nayak, 2000). Moreover, the M protein forms vesicles

and self-releases from cells when singly expressed from cDNA (Takimoto et al., 2001).

The fusion of SeV requires co-expression of both HN and F proteins. The HN and the F proteins are integral membrane glycoproteins and are essential for regulating morphogenesis and budding (Takimoto et al., 1998; Fouillot-Coriou and Roux, 2000). The HN protein is involved in cell attachment and is responsible for the adsorption of the virus to sialic acid-containing cell-surface molecules. In addition, it mediates enzymatic cleavage of sialic acid, namely neuraminidase activity, from the surface of virions and of infected cells. This activity prevents self-aggregation of viral particles during budding at the plasma membrane. The F protein mediates viral penetration by fusion between the virion envelope and the host cell plasma membrane. The F protein is synthesized as a precursor F0 which must be proteolytically cleaved to F1 and F2 for fusion activity (Morrison, 2003). The fusion occurs directly at the cell surface in an endosome-independent way, suggesting that infection does not require the acid pH of endosomes to activate fusion. The F protein has a self-release activity when expressed alone (Takimoto et al., 2001). After infection, the F proteins expressed on the plasma membrane of infected cells can mediate fusion with neighboring cells to form syncytia, a cytopathic effect that can lead to tissue necrosis *in vivo* and might be a mechanism of virus spread.

The P gene of SeV also expresses multiple accessory species of proteins by means of using overlapping open reading frames (ORFs) (Fig. 5), this gene encodes as many as eight polypeptides via these ORFs: the P, V, W, C′, C, Y1, Y2 and X proteins. SeV P gene mRNA contains 5 start codons near its 5' end, four of which are used for a nested set of "C" proteins that initiate at ACG^{81} (C'), AUG^{114} (C), AUG^{183} (Y1) and AUG^{201} (Y2) and terminate at UAA^{726}. Among the four C proteins, the C is the major species expressed in infected cells, at a molar ratio several fold higher than that of the other three

proteins (Kurotani et al., 1998). The second start codon, AUG^{104}, initiates 3 proteins (P, V and W) as a consequence of cotranscriptional mRNA editing (Lamb and Kolakofsky, 2001). The start site (AUG^{104}) for translation of the P protein is in a favourable context (kozak) for recognition by the ribosome; and since it is placed right after ACG^{81} (which is normally not a favourable start site) it is more often used. For SeV, AUG^{104}, and AUG^{114} are initiated by leaky scanning, whereas AUG^{183} and AUG^{201} are initiated by ribosomal shunting (Curran and Kolakofsky, 1988; Gupta and Patwardhan, 1988; Latorre et al., 1998b). SeV P gene contains an editing site in the middle of its reading frame. At this sequence, the vRNAP recognizes the 3'-UUU UUU CCC stretch on the template and occasionally stutters. This stuttering most likely occur when the vRNA pauses, and the growing RNA chain slips backward on the RNA template by one (or more) nucleotides (Pelet et al., 1991; Vidal et al., 1992; Hausmann et al., 1999). The vRNAP then resumes elongation. When this happens in the run of three G's, an extra G is added in the growing chain changing the reading frame. Addition of one G at the editing site produces an mRNA that encodes the V protein, whereas addition of two Gs leads to the W protein. The frequency of V and W production can vary depending on the kind of virus (Lamb and Kolakofsky, 2001).

1.3. Sendai virus life cycle

All aspects of the replication of SeV happen in the cytoplasm. In cell culture, single-cycle growth generally lasts for 24 hours. As the infection takes place, the virus is adsorbed to the receptors found at the cell surface, and fusion occurs between the viral membrane and the cellular plasma membrane. This leads to the release of the helical NCs in the cytoplasm. This NC containing the viral RNA genome is the template for all RNA synthesis (Lamb and Kolakofsky, 2001). Two functions are provided by the viral RNA genome: the mRNAs transcription and the viral RNA replication. The N,

P/C/V, M, HN and L proteins are synthesized by the cellular ribosomes. The assembly of the genomes and the N proteins takes place in the cytoplasm. The M protein lies in the inner surface of the cytoplasmic membrane whereas the HN and the F float at the membrane and concentrate to the M patches, excluding other cellular proteins. Finally, the NCs associate with the M proteins and the new viral particles bud out of the cell taking a portion of the plasma membrane (Lamb and Kolakofsky, 2001).

Intracellular replication begins with the transcription of the viral genome into capped and polyadenylated mRNAs by the vRNAP. The vRNAP first transcribes the leader RNA at the 3'end of the genome, and then begins the transcription of the genes into six individual mRNAs in a sequential and polar manner. This polymerase occasionally fails to reinitiate the downstream mRNA at each junction, leading to the loss of transcription of further downstream genes, consequently a gradient of mRNA synthesis that is inversely proportional to the distance of the gene from the 3'end of the genome is observed. The N protein is the most abundant of the structural proteins being synthesized, and the intracellular concentration of its unassembled state (N°) is a way of controlling the relative rates of transcription and the replication from the genome template. When sufficient amounts of N° are present, viral RNA synthesis becomes coupled to the concomitant encapsidation of the nascent (+) RNA chain. Under these conditions, vRNAP ignores all the junctions, to produce an exact complementary antigenome (+) chain, with fully assembled NCs. The anti-genome will then be used for the synthesis of a new RNA genome, which will be used again as a template or assembled into a nascent viral particle. The vRNAP can also initiate RNA synthesis at the 3'end of the antigenome in the absence of sufficient N, but only a trailer RNA is made in this case (Lamb and Kolakofsky, 2001).

1.4. Sendai virus strains

There are two known lineages of SeV: Z/H/Fushimi and Ohita M/Hamamatsu (Itoh et al., 1997; Fujii et al., 2002). The nucleotide sequences within each lineage are 99% identical and they are 89% identical between lineages. Z/H/Fushimi come from viruses isolated in Japan in 1956 after an epidemic of newborn infants and adapted to grow in embryonated chicken's eggs (Sakaguchi et al., 1994a; Itoh et al., 1997; Skiadopoulos et al., 2002). These adapted viruses, which were continuously passaged in eggs over a period of several decades are moderately virulent for mice (50% lethal dose [LD_{50}] = 10^3 to 10^4 PFU) (Sakaguchi et al., 1994a). Ohita M (SeVM) and Hamanatsu, in contrast, are highly virulent (LD_{50}, $<10^2$). They were both isolated from two completely separate, very severe epidemics of animal houses in Japan and were low-egg-"passaged". This virus is presumably closer to the virus in its natural host, and it is known that SeV passage in eggs attenuates its virulence in mice. For instance, in an infectious model, in which Kiyotani et al used three-year old mice, the Hamamatsu strain was very virulent; but when serially "passaged" 30 times in eggs, its strain became attenuated (Kiyotani et al., 2001).

2.0 Host–virus interface

2.1 Host defensive measures

Following respiratory tract infection, SeV proliferates extensively in the lungs reaching peak titers on the fourth to fifth day of the infection (Breider et al., 1987). Thereafter, virus titers decline rapidly with infectious virus no longer recoverable after the 10th–11th day post-infection (Brownstein and Winkler, 1986; Breider et al., 1987). Cellular immune responses are very important in the immunity against the viral infection. Local cellular accumulation has been documented as early as day 2 post-infection and cytotoxic T cells sensitized to SeV antigen can be detected in the spleen early in the infection with their activity reaching a peak on the sixth day. Virus-specific $CD8^+$T cells play an

important central role in the immune response, by recognizing the peptide antigens and triggering the specific lyses of virally infected cells (Chen et al., 1998). Even though it has been demonstrated that $CD4^+$T cells can also control the virus infection when ‘‘working’’ in synergism with $CD8^+$T cells (Zhong et al., 2001), they are mostly important in the regulation of antibody production, and in the control of a secondary virus infection (Zhong et al., 2000). The virus is also an excellent inducer of IFN (Brownstein and Winkler, 1986) as well as other cytokines such as interleukin 2 (IL-2), tumor necrosis factor (TNF), IL-6 and IL-10. Their peak titers are observed at the 7th to 10th day post-infection, about the time that the virus is cleared from the lung (Mo et al., 1995). Those cytokines are produced by $CD4^+$T cells, and also by $CD8^+$T cells but at lower levels, and they are able to decrease transcription and/or replication of the virus (Hou et al., 1992; Mo et al., 1995).

2.2 Virus defensive countermeasures

The ability to circumvent host response illustrates well a co-evolution of virus to overlap immune evasion. Viruses have evolved a variety of strategies to counteract the antiviral effects of IFN. These strategies falls into three categories, which are (i) functional inhibition of antiviral proteins, (ii) inhibition of IFN production and (iii) inhibition of IFN signaling. SeV fall into the third category, which so far has been mostly limited to DNA viruses. Indeed, the C proteins (C, C0, Y1 and Y2) expressed by the P gene by means of overlapping open reading frames, is responsible for blocking IFN signaling. SeV suppresses IFN-stimulated tyrosine phosphorylation of signal transducers and activators of transcription at an early phase of infection and further inhibits the downstream signaling. By this way, SeV C protein functions as an IFN antagonist and renders cells unresponsive to IFNα/ β and IFN-γ, counteracting the host immune defenses (Gotoh et al., 2001; Gotoh et al., 2003; Sakaguchi et al., 2003;

Kato et al., 2004). Once more, one can anticipate that the defensive countermeasures implemented by SeV offer clues to still unknown mechanisms shared by most *Paramyxoviridae*.

2.3 Susceptibilities to Sendai virus among inbred mice strains

Different susceptibilities among inbred strains of mice to SeV infection have been observed and confirmed by several authors (Itoh et al., 1989; Faisca et al., 2005) (Table 1.2). Generally, resistant strains of mice are known to repress the initial viral replication than susceptible strains. In addition, mice with resistant phenotypes abrogate the infection by confining infected regions primarily to the airways, whereas those with susceptible phenotypes allow the infection to spread from the airway into the lung parenchyma with severe pathological outcomes (Itoh et al., 1991; Faisca et al., 2005). Furthermore, immunodeficient mice or mice that were given immunosuppressive agents react to SeV in a different way than conventional mice. In these immuno-suppressed animals, the virus persists longer in the lungs, antibodies are produced later, recovery occurs later and the infection is no more restricted to the lungs, with contamination of the spleen, liver, and brain (Hou et al., 1992; Miyamae, 2005).

Table 1.2: Classification of Sendai virus susceptible inbred mice strains

Resistant strains	Susceptible strains
A/J	DBA/2
A/HeJ	DBA/2J
AKR/J	C3H/Bi
BALB/CJ	Nude (Swiss)
C57BL/6J	129/J
C57L/J	129/ReJ
C58/J	
C3Heb/FeJ	
RF/J	
SJL/L	
SWR/J	
Swiss[e] & Swiss[d]	

3.0 Genetic analysis of quantitative traits

The crossing of phenotypically different inbred strains enables the mapping of quantitative and qualitative trait loci. Analysis of a complex trait typically involves choosing phenotypically distinct parental strains, but these strains should also be genotypically distinct because genetic mapping depends on the polymorphic differences between parents. Genetic mapping studies can be performed in second-generation cohorts such as F2 and backcross. The phenotype observed in these progenies reflects the genetic re-assortment of the two parental strains and may reveal new genetic combinations that cause phenotypes diverse from the original observed on the parental strains.

Genetic inherited characters that can be easily classified into distinct phenotypic categories such as resistance/susceptibility to disease are considered to be qualitative traits and frequently can be studied according classical Mendelian analysis. However, a large part of the genetic inherited characters are measurable as a continuous variable, demonstrating large variation in the population and are considered to be quantitative traits showing complex patterns of inheritance. Such traits can be analyzed under the assumption that the phenotype in a given individual is quantitatively contributed by several loci, called quantitative trait loci (QTL). A number of statistical methods and study designs have been developed that have made it possible to determine the locations of QTL that control such traits. The identification of QTL is based on methods of linear regression of the phenotypic values on the genotype that allow inferring the variance explained by a given QTL (Camp and Cox, 2002). The chromosomal location of the QTL can be estimated using the interval-mapping method that calculates association of the trait to loci located between genetic markers. The maximum likelihood of odds (LOD-score analysis) or likelihood ratio statistics (LRS) for a QTL at each point can then be estimated and plotted against a

framework linkage map.

The standard approach for mapping QTL contributing to variation in a quantitative trait makes use of the assumption that the variation follows a normal distribution in the population in question (Lander and Kruglyak, 1995). However, many quantitative traits of interest are not normally distributed. Recently a number of attempts have been made to develop genetic models that allow the analysis of non-normal distributed quantitative traits as is the case of the parametric two-part model and the non-parametric model (Broman et al, 2003).

The parametric two-part model is designed for analysis of quantitative traits that show a spike in the distribution. If the proportion of individuals within the spike is appreciable and the phenotype is well separated from the rest phenotypic distribution, the normal model of QTL mapping has a tendency to produce false LOD score peaks in regions of low genotype information. To circumvent this problem the two-part model considers two separated maximum-likelihood estimations: the analysis of the quantitative phenotype by standard interval mapping using only the individuals within the normal distribution and the analysis of the binary trait that considers the individuals in the spike against the remaining individuals (Broman 2003). The resulting LOD-score is simply the sum of the LOD scores from the two separate analyses.The nonparametric model applicable for non-normal distributions considers a rank-based analysis of the phenotype. Each individual is represented by a rank value and the average rank for each genotype category is then compared using a Kruskal-Wallis statistic test (Broman et al, 2003). This nonparametric statistics follows approximately a chi-square ($\chi 2$) distribution under the null hypothesis of no linkage and can be mathematically transformed into a LOD score (Broman et al, 2003).

4.0 PART 1

4.0 Genetic analysis of Sendai virus infection in mice

4.1. Introduction

Sendai virus (SeV), the murine counterpart of human parainfluenza virus type 1 (HPIV1), is a natural respiratory pathogen of mice, which is highly related both structurally and serologically to HPIV1 that causes severe respiratory disease in children with the increasing risk of asthma. The virus belongs to the *Paramyxoviridae* family which remains endemic and it is the leading cause of pneumonia among rodent's colonies in various laboratories world wide; hence the concepts of specific pathogen-free laboratory animals (Chanock, 2001). Recently, it has been reported that the virus was able to replicate in the upper and lower respiratory tract of chimpanzees and African green monkeys and therefore may cause zoonotic disease in humans (Skiadopoulos et al., 2002). Furthermore, the virus has been used extensively in research studies that define most of the basic biochemical and molecular biological properties of *Paramyxoviruses* (Fascia and Desmecht, 2007), and experimental infection of mice with SeV is frequently used to study the viral pathogenesis of human respiratory diseases (Kim et al., 2008). In mice, generally resistant strains are up to 20,000-fold more resistant to the lethal effects of SeV than susceptible strains. In addition, mice with resistant phenotypes abrogate the infection by confining infected regions primarily to the air ways, whereas those with susceptible phenotypes allow the infection to spread from the air way into the lung parenchyma (Brownstein and Winkler, 1986; Itoh et al., 1991; Fascia et al., 2005). The two inbred mice, DBA/2 (D2) and C57BL/6 (B6), differ markedly in the susceptibility to SeV infection. For instance, infected B6 mice have 10-300 times lower viral titers than

D2 mice and the virus replicates predominantly in air epithelial cells which causes the inflammation of airways. In addition, B6 mice mount vigorous IFN response and less severe pulmonary pathology. In contrast, D2 mice fail to mount augmented IFN and natural killer (NK) cell response, thereby leading to the spreading of the lesions into the lung parenchyma and massive replication of the virus in alveolar lining cells (Itoh et al., 1991; Baig and Fish, 2008) Earlier reports based on genetic differences generated an array of hypotheses about associated phenotypic characteristic (sex and coat colour) or underlying gene polymorphisms such as IFN, mucocilliary transport or *Sas-1*, TLR, and H-2 haplotype, none of which fully confirmed the genetic basis of the varying spectrum of resistance and susceptibility to SeV (Brownstein and Winkler, 1986; Breider et al., 1987; Hou et al., 1992; Mo et al., 1995; van der Sluijs et al., 2003). Since resistance and susceptibility to infection is complex genetic trait, and as a step towards the elucidation of the contributing genetic host factors for SeV infection in mice, in this study, the author exploited the contrasting response of inbred D2 and B6 to SeV infection and carried out the genetic mapping studies in these two mouse strains with the goal of dissecting these genetic variants, which might provide valuable insights into the molecular basis of host variations to SeV infection.

4.2. Materials and Methods

4.2.1. *Design*

Two hundred and fifty Microsattelite markers that showed polymorphism between B6 and D2 mice were screened, and 100 markers were selected for the genotyping analysis, with an average genetic distance of 10.0 cM using the MGI data base. Subsequently 25 additional markers were added to localized loci of interest.

Two independent experiments were carried out with 34 mice from each of the two strains (B6 and D2) at 8 weeks of age, with equal number of males and females, all mice were inoculated intranasally with SeV inoculums at different viral concentration of tissue culture infectious dose [1×10^2 $TCID_{50}$, 1×10^3 $TCID_{50}$, 1×10^4 $TCID_{50}$ and 1×10^5 $TCID_{50}$] for a post infection period of 21days. This was followed by subsequent infection of parental progenies with 1×10^3 $TCID_{50}$ as the choice dose that discriminated between the two parental (B6 and D2) strains.

4.2.2. *Animals*

Specific pathogen-free B6 and D2 mice were purchased from Sankyo Laboratories Service Cooperation INC (Hamamatsu), Japan. Mice from both parental strains were bred and raised under bio-clean and regulated conditions, of the bio-safety level 3 Animal facility of the Graduate School of Veterinary Medicine, Hokkaido University, Japan. All experimental protocols were approved and carried out according to the guidelines for the Care and Use of Laboratory Animals and the Institutional Animal Care and Use Committee of the Graduate School of Veterinary Medicine, Hokkaido University.

4.2.3. *Infection*

Seed virus stock in modified Eagle medium (Sigma, MO, USA) with 1% bovine serum albumin

was inoculated into 10-day-old embryonated chicken eggs and incubated for 72 h at 35 ^{o}C. After allantoic fluid recovered from inoculated eggs was centrifuged at 2,500 x g for 20 min, the supernatant was collected and stored at - 80^{o}C until used for infection to mice. Virus titer in the allantoic fluid was determined by hemadsorption assay using a monkey kidney cell line, LLC-MK2, and chicken red blood cells. The values of virus titer were indicated as median tissue culture infectious dose ($TCID_{50}$).

Mice were infected using 1×10^{3} $TCID_{50}$ of SeV, 25 µl of the viral innoculum was slowly instilled intranasally, following inhalation anesthetization with Methoxyflurane (Abbott Co LTD, Japan) and/or intra-peritoneal injection of Somnopentyl® (Schering-Plough Animal Health NJ, USA). DBF_1, DBF_2 and DBN_2 mice were generated to conduct the genetic breeding studies. The female parent used for generating intercross and backcross mice was D2. For the determination of virulence, infected mice were weighed daily and monitored by visual inspection twice per day, with the main visual disease signs being lethargic, ruffled fur, hunching and with evident of dyspnea. Mice were sacrificed by cervical dislocation if the weight loss exceeded 40% of the weight from day 0 or if the animals were obviously in the extremis.

4.2.4. *Genotyping analysis*

Genomic DNA was prepared from tail snips of parental strains and backcross progenies. Tails were incubated at 55 ^{O}C for 16-24 h in 500 µl of lysis Buffer [10 mM Tris-HCL (pH 8.0), 150 mM NaCl, 10 mM EDTA (pH 8.0) and 1% Sodium dodecyl sulfate (SDS)] together with 100 µg of Proteinase K and RNase solutions. This is followed by standard phenol chloroform extraction and finally genomic DNA was purified by ethanol precipitation in the presence of 0.3 M sodium acetate and resolved in TE buffer [10 mM Tris-HCL and 1 mM EDTA (pH 8.0)].

4.2.5. *Microsattelite markers*

To identify and map QTL, a total of 125 informative MIT Microsattelite markers were used for the genotyping analysis. Initially we genotyped a set of 100 markers, that differentiated between the allele of B6 and D2 mice. The genetic map positions (cM) and physical map positions (Mb) of markers loci were obtained from the Mouse genome data base (MGD) of the Jackson Laboratory (http://www.informatics.jax.org/). We typically typed at least four markers per chromosome, which provide an average genome scan radius of approximately 10.0 - 20.0 cM selected to provide coverage of all 19 autosomes and the X chromosomes (Table 1.3). However, additional 25 markers were added at chromosomal regions of interest to estimate the QTL positions more precisely.

4.2.6. *Amplification of microsattelite markers*

DNA (100 ng) samples from parental strains and that of the progenies were amplified using the PCR thermal cycling sequence parameters of 94 ^{O}C for 4 min (one cycle). This was followed by 40 cycles consisting of denaturing at 94 ^{O}C for 40 s, primer annealing at 55 ^{O}C for 30 s and extension at 72 ^{O}C for 30 s. PCR mixture and enzyme (Taq DNA polymerase) were purchased from (TaKaRa Bio Inc Tokyo, Japan). The amplified samples were electrophoresed with 9% polyacrylamide gels in 1×TBE and stained with ethidium bromide. The stained gels were then visualized and photograph under ultraviolet lamp. For each marker the two genotypes could be distinguished unambiguously and touchdown PCR protocol was used to improve the specificity of annealing.

4.2.7. *Linkage and statistical analysis*

For the genome scans, only two phenotypic categories, 40% body weight loss (value = 0) and less than 40% body weight loss (value = 1) were used as survival phenotype of mice. Analyses of

linkage of percentage body weight loss as survival phenotypes to autosomal loci were performed using the MapManager QTXb20 (Manly et al 2001) a program that uses a maximum likelihood alogorithm with “interval mapping” and “simultaneous search”, and permits better localization of loci and exclusion mapping. Recombination frequencies (%) were converted into genetic distance (in cM) using the Kosambi map function. This program provides linkage data as likelihood ratio statistic (LRS) score and it has been converted to the more frequently used LOD score by dividing the LRS by 4.601. The values for free, dominant and additive models of inheritance were calculated in terms of LRS by carrying 5,000 permutations. The threshold in the backcross progenies under the assumption of a free model were LRS > 6.8 and LRS > 12.5 for suggestive and significant linkages respectively.

Two-way interactions (epistasis) were estimated with a QTL can and statistical significance for these gene to gene interaction tests were based on $P < 0.05$ using 5,000 permutations of the observed data. Significant interactions found in the QTL were confirmed with standard ANOVA, including cross terms for two-way interactions for all maker pairs. All computations were performed with the Stat view program statistical package (SAS Institute, Cary, NC). $P < 0.05$ was considered to be significant.

4.3 Results

4.3.1 *Determination of the genetic spectrum and mode of resistance and susceptibility to Sendai virus*

Inbred strains of mice with different susceptibilities to SeV infection have been identified previously. B6 and D2 mice differ markedly in response to SeV infection. Percentage body weight changes and survival times were chosen as parameters for the evaluation of SeV resistance and susceptibility phenotype for an infection period of 21 days. Initially the author tested the spectrum of sensitivity of D2 and B6 mice, by challenging them at different viral titer levels of $TCID_{50}$ of SeV inoculums. In a two independent experiments, mice (males and females, n= 4–5) were inoculated intra-nasally with SeV inoculums, with dose ranges of 1×10^2, 1×10^3, 1×10^4, and 1×10^5 $TCID_{50}$. All of mice showed obvious signs of infection between 3 and 5 days, of which they appear to be lethargic, ruffled fur, hunching, dyspnea, and loss of weight (Percy et al., 1994). D2 showed a progressive loss of percentage body weight and mortality in all dose ranges, while B6 mice showed slight loss of body weight which returned to normal and only 10% mortality even at very high virulent dose of 1×10^5 $TCID_{50}$. In addition, resistance and susceptibility were not linked to sex. These results reconfirmed the earlier reports on differences in the spectrum of susceptibility to SeV between these two strains (Brownstein and Winkler, 1986; Itoh et al., 1991). In order to investigate the mode of resistance to SeV, we infected parental strains in replicate experiments (males and females, n= 17) with 1×10^3 $TCID_{50}$, of which dose clearly discriminated between susceptible D2 and resistant B6 mice and served as a choice dose for our genetic mapping studies. In addition, as a control for each analysis, groups of D2 were infected at the same time as the DBF_1, DBF_2, and backcrossed progenies. D2 mice showed a progressive loss of weight and mean survival time was 10.0 ± 1.0 days for females and 9.0 ± 1.5 days for

males, while B6 mice (male and females) from day 0, showed approximately 20% decline in body weight between day 6 and 7, and by day 8 they started regaining weight which returned to normal with a 100% rate of survival (Fig 1.4) Thus, these results indicate that B6 has a conferred genetic molecular mechanism of abrogating the infection. Therefore, the author investigated the genetic inheritance of resistance and susceptibility of DBF_1 mice. In two independent experiments, 16 DBF_1 mice were tested (males and females) using 1×10^3 $TCID_{50}$ (Fig 1.4). Interestingly, DBF_1 mice were more resistant than both parental strains and they showed approximately 15% decline in percentage body weight loss between day 6 and 7, and survival rate was 100%. In addition, we also found that resistance was not sex-dependent, but remained dominant.

4.3.2 *Phenotypic characterization of Sendai virus resistance and susceptibility*

To estimate the effect of genetic trait of SeV susceptibility, segregation analysis was performed. The null hypothesis was that a single dominant gene controls resistance. If so, then according to Mendelian rule, 100% of the F_1 hybrid of resistant B6 strain crossed to sensitive D2 strain should display a resistant phenotype and 50% of the backcrossed mice of the F1 hybrid crossed to sensitive D2 should be resistant. Chi-square analysis of the DBF_1 response supported the null hypothesis ($\chi^2 = 0.22$, $P < 0.05$). Furthermore, 61/ 108 (56.5%) of the backcrossed DBN_2 mice were resistant, which agrees with predicted 50% according to the Mendelian rule. However, chi-square analysis of DBF_2 mice, however, rejected the null hypothesis ($\chi^2 = 23.34$: $P > 0.05$), suggesting that sensitivity to SeV is a muligenic trait control by several loci within the mouse genome.

4.3.3 *Linkage analysis for the identification of genetic loci of Sendai virus resistance and susceptibility*

To investigated the resistance and susceptibility phenotype of the progenies of DBN_2 mice. The author used backcrossed progenies for genetic analysis, because the phenotypes of DBF_1, mainly the loss of body weight showed a dominant genetic trait. This allows for optimal discrimination between the phenotypes recovered in the backcrosses. A total of 108 (54 males and 54 females) backcrossed mice were infected with 1×10^3 $TCID_{50}$ SeV and phenotypes of body weight change were determined as QT. Alternatively, the susceptible or resistant phenotype was determined as 40% body weight loss or less than 40% body weight loss, respectively, because these phenotypes were consistent with susceptible (non-survival) or resistant (survival) phenotype in the pilot study. A simple interval mapping was carried out and the values for the free, dominant, and additive models of inheritance were calculated in terms of LRS. When percentage body weight loss was used as QT, none of significant or suggestive QTL was detected. Therefore, 40% body weight loss (value = 0) or less than 40% body weight loss (value = 1) was used as QT, and linkage analysis revealed a major significant QTL, which mapped to the distal region of Chr 4, residing within 8.3 cM (23 Mb) between *D4Mit146* and *D4Mit20*4 (LRS 14.5), denoted as *SeV1* locus (Fig 1.5). Additional QTL showing suggestive linkages were also detected on Chr 8 (between *D8Mit4* and *D8Mit100*, LRS 8.4) and 14 (between centromere and *D14Mit10*, LRS 7.4), $P < 0.005$ (Fig 1.5).

4.3.4 *Identification of epistatic interaction involved in Sendai virus resistance and susceptibility*

Epistatic interactions results from the combined effect of two or more genes on a phenotype, which could not have been predicted as the sum of their separate effects (Frankel and Schork, 1996). Recent evolutionary trends have shown that in crosses involving a strain of model organism susceptible to certain disease conditions with resistant strains, the genes of the susceptible strain show differential

effects with the different background strain genomes (Rapp et al., 1994). Based on the hypothesis of the genetic background and evolutionary evidence of gene to gene interactions, the author investigated the possibilities of epistatic interactions by performing ANOVA of all informative markers in 108 DBN_2 progenies using Stat view program statistical package (SAS Institute, Cary, NC). All informative pairs of markers were tested one by one, with a *P* value of <0.05 as the threshold for finding gene to gene interactions. The analysis also includes both the previously identified significant and suggestive QTL, and at the set *P* value threshold we identified a highly significant epistatic interaction between *D3Mit182* and *D14Mit10*, $P < 0.0001$ (Fig 1.6A). Thus, *D14Mit10* is one of the previously identified suggestive QTL (Fig 1.5) and it is interacting epistastically with a locus on Chr 3 (*D3Mit182*), therefore denoted as *SeV3* and *SeV2* loci, respectively (Fig 1.6, Table 1.4). Finally, the author interrogated our likely candidate region of the QTL on Chr 4, *SeV1*, which showed a peak level on *D4Mit308*, and carried out a mean survival rate analysis of mice with respect to genotype at this locus. A single genotyping analysis at this locus revealed a mean survival rate of 66% for heterozygous (B6/D2 allele) and 34% for homozygous (D2 allele) (Fig 1.7A). Next, addition of the effect of the suggestive interacting locus, *SeV3* (*D14Mit10*), revealed a novel increase in survival rate, with the B6/D2 allele mice with respect to both *D4Mit308* (*SeV1*) and *D14Mit10* (*SeV3*) loci having 74% mean survival rate, while mice carrying D2 allele at both loci had 14% mean survival rate (Fig 1.7B). Therefore, the author went ahead to include the locus effect that showed epistatic interaction by fixing *D3Mit182* (*SeV2*) to be heterozygous, and carried out an estimation of mean survival rate with genotypes at the above two loci. Cumulatively, 93.3% of heterozygous mice were resistant to SeV infection, whereas homozygous mice showed a value of 0% survival rate (Fig 1.7C), indicating the combined effects of the significant QTL and the loci

showing highly significant epistatic interaction in the control of resistance to SeV infection. Thus, these data revealed that there could be several genetic factors that are localized within the mouse genome regulating the differential sensitivity of these mice to SeV infection.

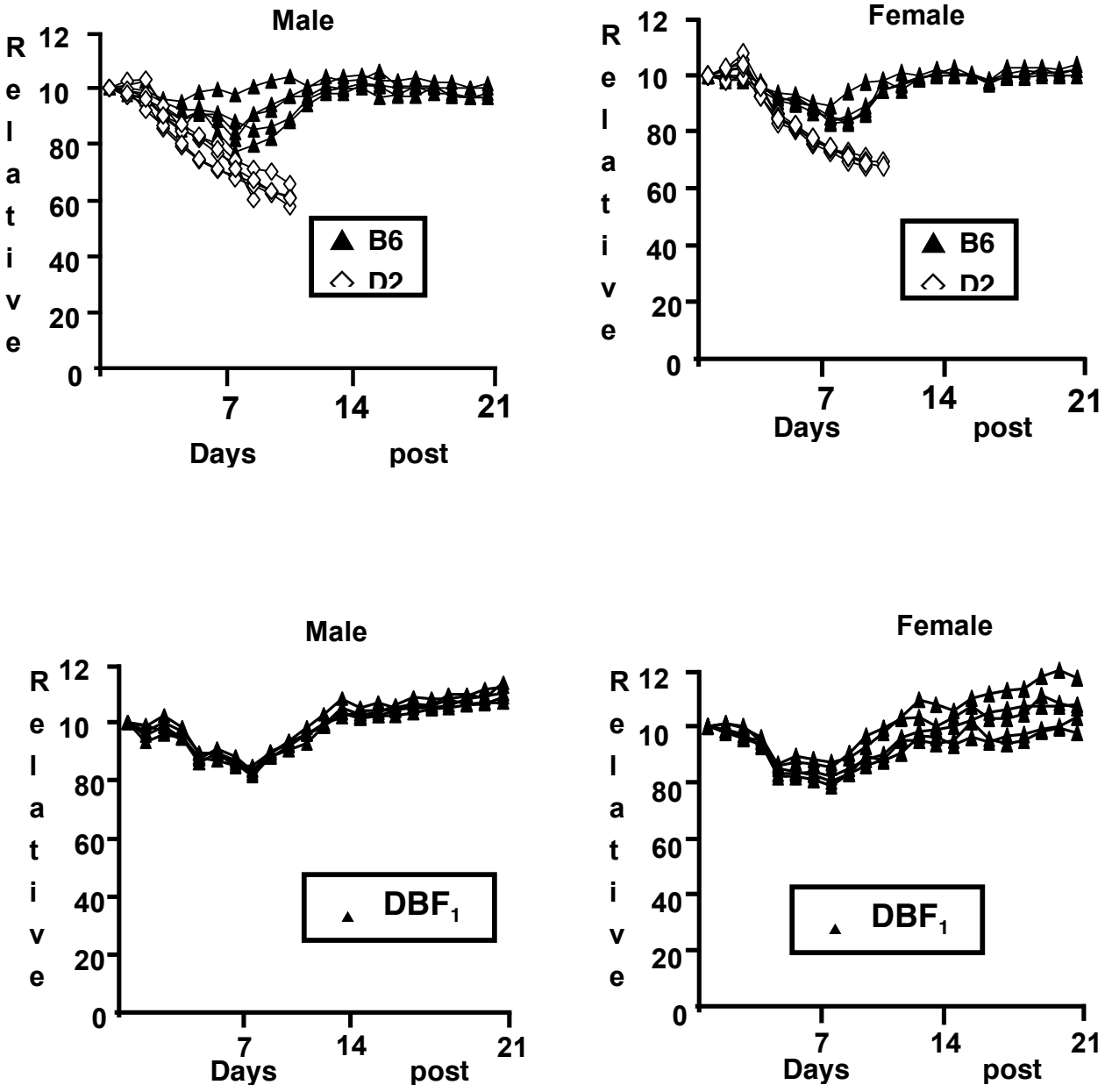

Fig 1.4. The time course and body weight changes as relative values following SeV infection. Sensitivity to SeV infection between parental strains and DBF1 mice was determined. Relative body weights are presented as percent of initial body weight before viral inoculation for individual mouse. Initial body weights for each group were as follows: male D2, 20.4 ± 0.6 g; female D2, 21.0 ± 0.4 g; male B6, 20.0 ± 0.1 g; female B6, 20.0 ± 0.9 g; male DBF1, 23.3 ± 0.5 g; female DBF1, 22.1 ± 0.7 g.

Table 1.3. List of microsatellite markers used for the QTL analysis.

Microsatellite Markers	cM	Microsatellite Markers	cM	Microsatellite Markers	cM	Microsatellite Markers	cM	Microsatellite Markers	cM
D1Mit118	8.3	*D4Mit178*	35.5	*D7Mit66*	57.5	*D11Mit212*	50	*D15Mit161*	69.2
D1Mit1002	16.0*	*D4Mit152*	40	*D7Mit333*	66	*D11Mit199*	62	*D16Mit182*	3.4
D1Mit324	32.1	*D4Mit327*	42.5	*D8Mit4*	14	*D11Mit48*	77	*D16Mit59*	27.8
D1Mit415	52	*D4Mit186*	44.6	*D8Mit100*	31	*D12Mit219*	6	*D16Mit140*	42.8
DI Mit191	64	*D4Mit303*	48.5	*D8Mit261*	32.5	*D12Mit172*	22	*D16Mit152*	57
D1Mit14	81.6	*D4Mit146*	53.6	*D8Mit31*	33	*D12Mit5*	37	*D16Mit86*	66
D1Mit291	101.5	*D4Mit308*	57.4	*D8Mit234*	37.3	*D12Mit101*	50	*D16Mit106*	71.5
D2Mit293	11	*D4Mit204*	61.9	*D8Mit242*	47	*D13Mit17*	8	*D17Mit113*	6.5
D2Mit296	18	*D4Mit54*	66	*D8Mit200*	58	*D13Mit60*	16	*D17Mit135*	17
D2Mit91	37	*D4Mit42*	81	*D9Mit90*	9	*D13Mit63*	26	*D17Mit89*	36
D2Mit185	47.5	*D5Mit180*	10	*D9Mit91*	17	*D13Mit9*	45	*D17Mit187*	47.4
D2Mit62	65	*D5Mit108*	26	*D9Mit302*	35	*D13Mit148*	59	*D17Mit221*	56.7
D2Mit286	87	*D5Mit258*	41	*D9Mit133*	43	*D13Mit262*	68	*D18Mit132*	11
D2Mit229	99	*D5Mit208*	54	*D9Mit355*	53	*D14Mit10*	3	*D18Mit17*	20
D2Mit200	107	*D5Mit188*	64	*D9Mit18*	71	*D14Mit120*	12.5	*D18Mit124*	32
D3Mit164	2.4	*D5Mit370*	70	*D10Mit248*	7	*D14Mit102*	28.3	*D18Mit184*	41
D3Mit182	23.3	*D5Mit222*	82	*D10Mit61*	32	*D14Mit225*	42.5	*D18Mit7*	50
D3Mit28	43.6	*D6Mit159*	7	*D10Mit186*	40	*D14Mit165*	52	*D19Mit69*	6
D3Mit14	64.1	*D6Mit74*	20.5	*D10Mit264*	50	*D14Mit170*	63	*D19Mit80*	22
D3Mit129	84.9	*D6Mit188*	32.5	*D10Mit14*	65	*D14Mit266*	60	*D19Mit89*	41
D4Mit235	1.9	*D6Mit150*	51	*D10Mit297*	70	*D15Mit12*	4.7	*D19Mit33*	53
D4Mit172	8.6	*D6Mit15*	74	*D11Mit226*	1.55	*D15Mit226*	11.6	*DXMit166*	15.5
D4Mit237	13.3	*D7Mit114*	8	*D11Mit21*	20	*D15Mit5*	22.2	*DXMit62*	34.6
D4Mit214	17.9	*D7Mit82*	25	*D11Mit140*	28	*D15Mit156*	39.1	*DXMit130*	55
D4Mit139	28.6	*D7Mit318*	37	*D11Mit4*	37	*D15Mit159*	49.6	*DXMit186*	69

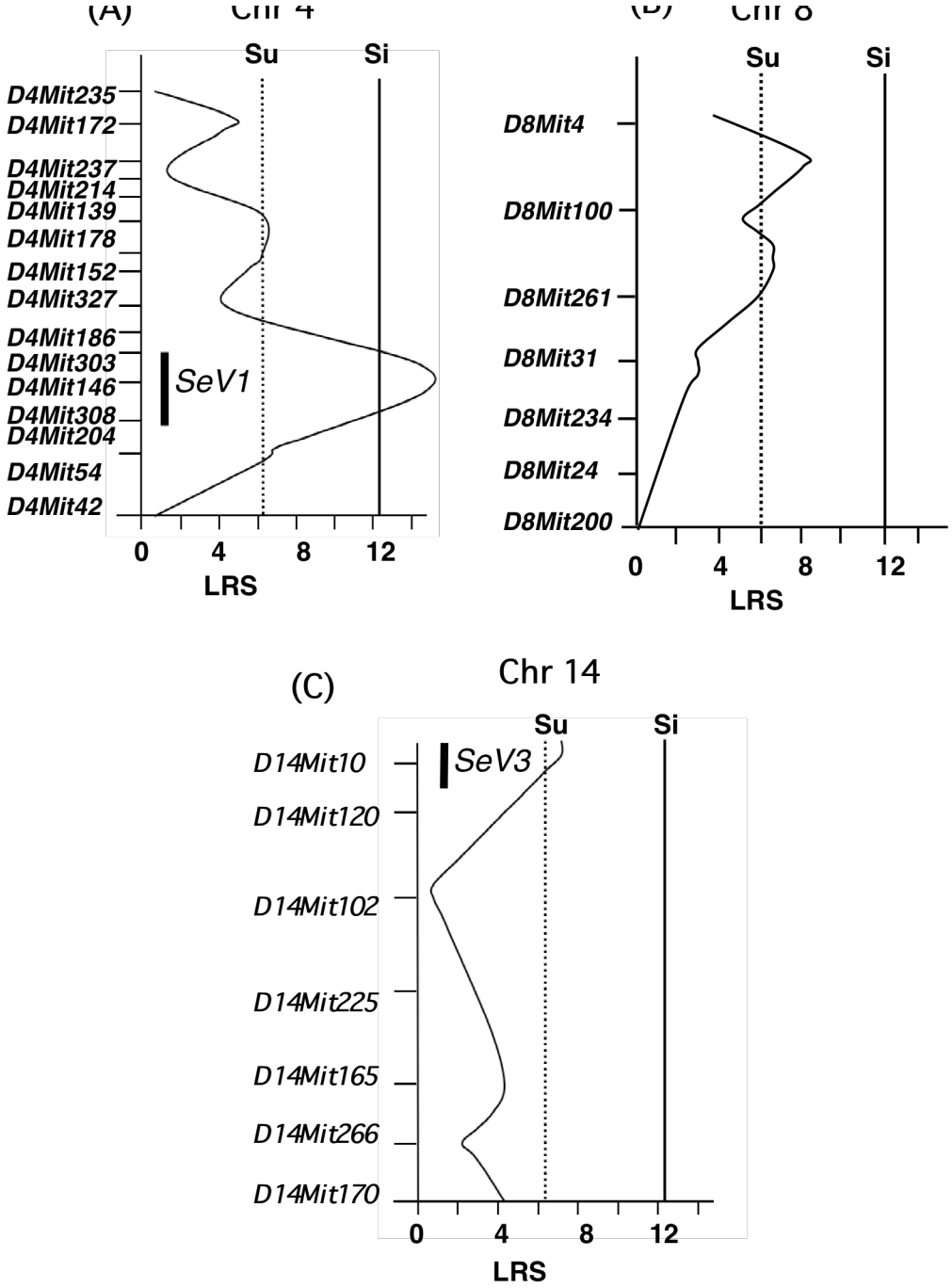

Fig 1.5. QTLs affecting SeV resistance and susceptibility in backcrossed progenies. Each vertical axis represents the genetic map for the mouse chromosome and the markers at which genotypes were determined. The threshold in the backcrossed progenies under the assumption of a free model were LRS 6.8 and 12.5 for suggestive (Su, dotted line) and significant (Si, solid line) linkages, respectively ($P < 0.05$). (A) *SeV1* was defined by a peak LRS value of 14.5 on Chr 4 observed at a confidence interval of 8.3 cM (24 Mb) extending from *D4Mit146* to *D4Mit204*, while Chr 8 (B) and 14 (C) showed suggestive loci. Suggestive QTL on Chr 14 was denoted as *SeV3*, because it showed a significant epistatic interaction with another locus (see Fig. 3).

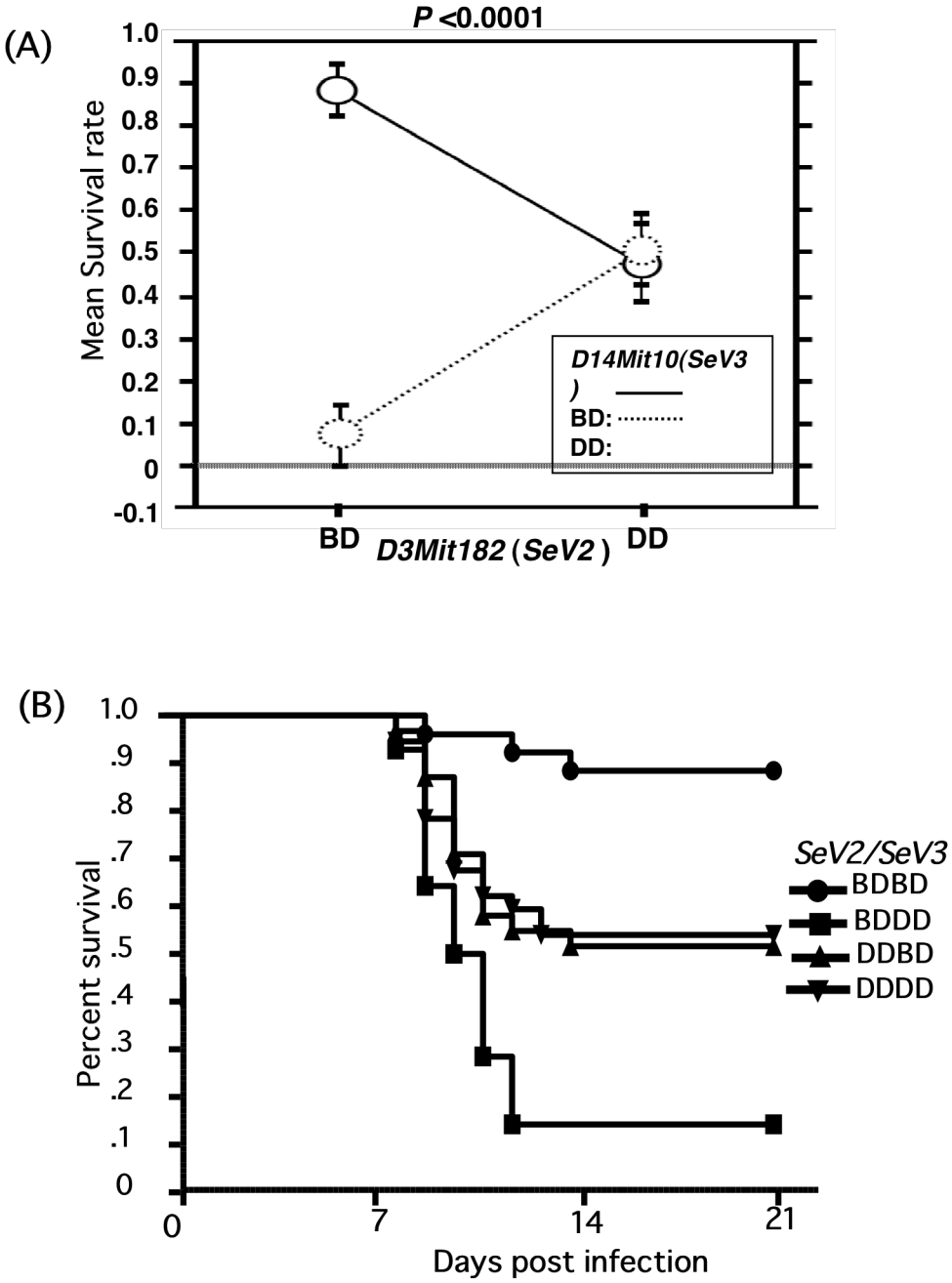

Fig 1.6. Epistatic interaction affecting SeV resistance and susceptibility in backcrossed progenies. (A) Plot of pair-wise interaction for the least square analysis of variance of all informative markers in 108 backcrossed progenies showed a highly significant epistatic interaction between *D3Mit182* and *D14Mit10*, $P < 0.0001$ and percentage of trait variance accounted for. Both loci were denoted as SeV2 and SeV3, respectively. Error bars represent standard error. (B) Kaplan–Meier plot of SeV-infected backcrossed mice with respect to their genotypes of *SeV2* and *SeV3* loci, which show epistatic interaction. In both (A) and (B), the survival rate was determined as the rate of mice showing less than 40% body weight loss after SeV infection in the light of ‘‘humane endpoint’’ concept.

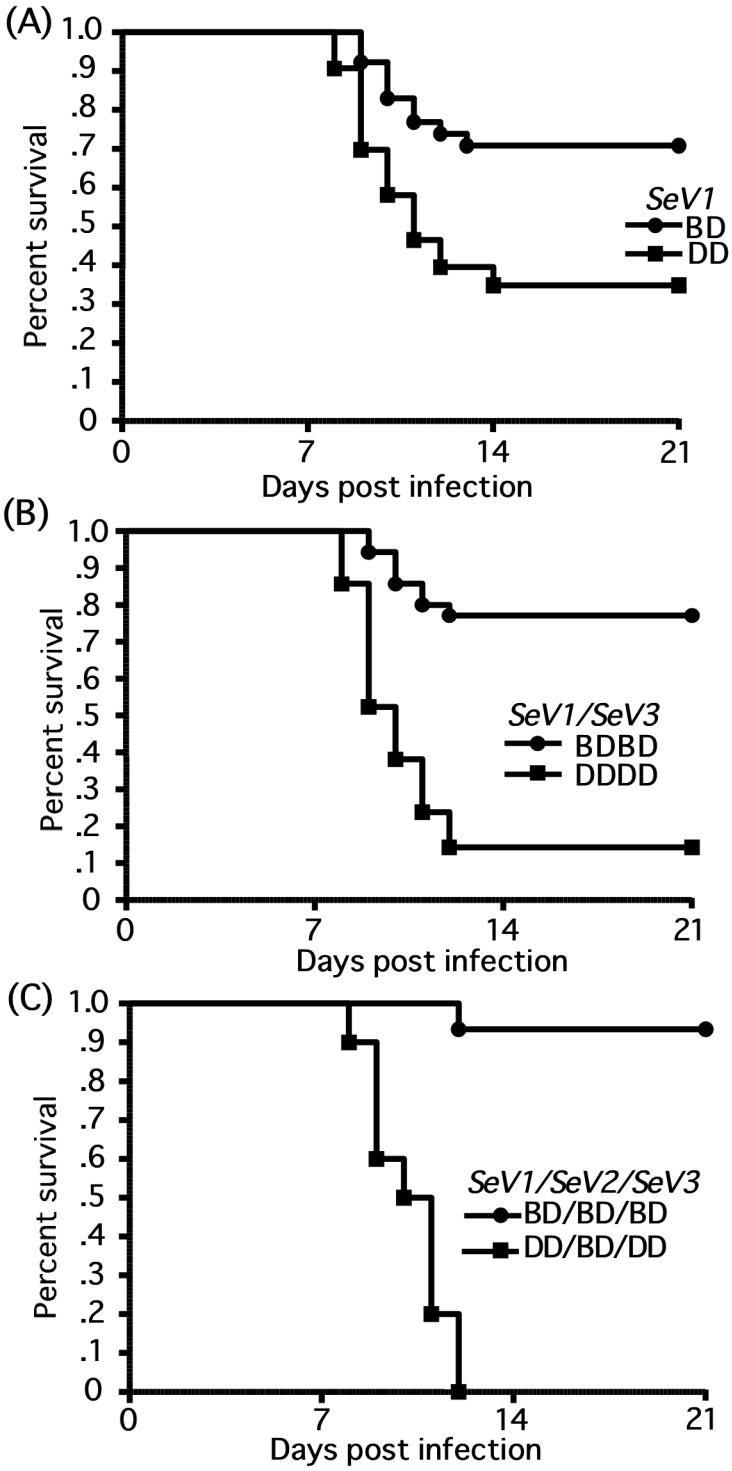

Fig. 1.7. Kaplan–Meier plot of SeV-infected backcrossed mice with respect to their genotypes of SeV1, SeV2, and SeV3 loci. (A) Kaplan–Meier plot of mice possessing heterozygous or homozygous with respect to *SeV1*. (B) Kaplan–Meier plot of mice with respect to *SeV1* and *SeV3*. (C), Kaplan–Meier plot of mice with respect to *SeV1*, *SeV2*, and SeV3. In this analysis, SeV2 (D3Mit182) is fixed to heterozygous to show epistatic interraction. In (A), (B), and (C), the survival rate was determined as the rate of mice showing less than 40% body weight loss after SeV infection in the light of ‘‘humane endpoint’’ concept.

Table 1.4. List of candidate genes for *SeV1*, *SeV2*, and *SeV3*.

Gene symbol	Gene description	cM
SeV1 candidates on Chr 4		
D4Mit146	Flanking marker	109.0
Faf1	Fas-associated factor 1	109.3
Tal1	T-cell acute lymphocytic leukemia 1	114.6
Im2	Immunoregulatory 2	114.6
Ptprf	Protein tyrosine phosphatase receptor F	117.7
Mpl	Myeloproliferative leukemia virus oncogene	118.1
D4Mit308	Significant locus	123.8
Csf3r	Colony stimulating factor 3 receptor	125.7
Tlr12	Toll-like receptor 12	128.3
Lck	Lymphocyte protein tyrosine kinase	129.2
Ptafr	Patelet-activating factor receptor	131.8
D4Mit204	Flanking marker	132.9
SeV2 candidates on Chr 3		
D3Mit164	Flanking marker	7.5
Il7	Interleukin 7	7.6
Tnfsf10	Tumor necrosis factor superfamily 10	27.2
Il2	Interleukin 2	37.0
Il21	Interleukin 21	37.1
Fgf2	Fibroblast growth factor 2	37.2
D3Mit182	Interacting locus	50.4
Il12a	Interleukin 12a	68.5
Pgdfc	Platelet-derived growth factor, C polypeptide	80.8
Tlr2	Toll-like receptor 2	83.6
Il6ra	Interleukin 6 receptor, alpha	89.7
D3Mit28	Flanking marker	90.4
SeV3 candidates on Chr 14		
D14Mit108	Flanking marker	13.1
D14Mit10	Suggestive and interacting locus	13.3
Rthyd3	Resistance to thymic deletion 3	13.4
Il3ra	Interleukin 3 receptor alpha chain	15.2
Il17rd	interleukin 17 receptor D	27.9
I17rb	Interleukin 17 receptor B	30.8
D14Mit120	Flanking marker	36.9

4.4 Discussion

One of the major challenges of modern biology is to achieve a better understanding of the molecular genetic basis for complex trait variation. Complex genetic traits are derived from the interplay between genetic variants and environmental exposures (Zondervan and Cardon, 2004), where a one-to-one relationship between genotype and phenotype does not exist (Darvasi, 1998). SeV infection in mice, like many diseases and biological phenotypes, is thought to arise as a consequence of the interplay of two or more genes.

Earlier reports have shown that there is differential sensitivity to SeV among various inbred mouse strains. SeV-infected B6 mice elicit a strong IFN and $CD4^+$/$CD8^+$ T cell response in the respiratory tract and it is believed that they have a coordinated interaction for the effective clearance of SeV in these mice; however, whether they act directly to eliminate the virus-specific response is not clear. Adoptive transfer studies suggest that $CD4^+$ T cells may contribute to the B6 anti-SeV response by providing help to cytotoxic T cells in the form of IL-2 (Kast et al., 1986; Hou et al., 1992; Cole et al., 1994). Lopez et al. (2006) have shown that type I IFNs facilitate virus clearance and enhance the migration and maturation of dendritic cells after SeV infection *in vivo* soon after infection. However, mice cleared the virus from their lungs and efficiently generated cytotoxic T cells independently of type I IFN signaling. Furthermore, mice that are unresponsive to type I IFN developed long term anti-SeV immunity, including $CD8^+$T cells and antibodies. Recently, Kim et al (2008) have shown that wild type B6 mice no longer have detectable viral titer and a trace level of SeV-specific RNA expression after infection and that macrophages derived from these mice express IL-13 mRNA. Further, the analysis of macrophage-deficient mice (*Csf3*-/-) indicates that both IL-13 and mucin 5ac production after SeV

infection depends on the presence of macrophage. Furthermore, it is believed that both host and viral factors play a role in the resistance and susceptibility to SeV virus, and the activation of innate immune system depends on the recognition of the molecules that are specific for the pathogen. For instance, for the *Paramyxoviridae*, the anti-host defense mechanism is due mostly to C and V proteins. SeV C protein is a multifunctional protein that plays important roles in regulating viral genome replication and transcription, antagonizing host IFN system, suppressing virus-induced apoptosis, and facilitating virus assembly and budding. Similarly, the V protein is shown to participate in the establishment of antiviral state that is required for viral pathogenesis (Kato et al., 1997, 2007; Garcin et al., 2000; Strahle et al., 2003).

Host response to SeV infection involved complex interactions of a number of factors, including cellular infiltration and their induction of chemokines (Kast et al., 1986; Mo et al., 1995; Strahle et al., 2007). However, the definition of this host response to SeV infection will require an understanding of the host genetic susceptibility to the virus. In this study, QTL analysis was performed to examine differences in SeV sensitivity between inbred D2 and B6 mice. The identification of clear phenotypes of resistance and susceptibility to SeV is a valuable tool for genetic analysis in mice. The author carried out a QTL analysis on body weight loss in backcrosses from D2 and B6 mice after infection with SeV. These two mouse strains represent polar extremes in severity of SeV-triggered disease (Fig. 1.4), which in addition to the rate of body weight loss, is manifested by several phenotypes previously identified. These phenotypes include mean survival time, viral loads as well as histopathology of the lungs (Itoh et al., 1991; Percy et al., 1994; Faisca et al., 2005). However, the abrogation of early onset of SeV-induced loss of weight in backcrossed mice is the most attractive phenotype for analysis, because of

its ease of accurate determination. One interesting phenomenon was the mode of inheritance for the sensitivity to SeV infection. The phenotypes of weight loss of the DBF_1 progenies of D2 cross to B6, as well as in DBF_2 mice demonstrate that resistance is inherited as a dominant trait. The results from DBF_2 mice after infection suggest that multiple genes influence susceptibility to SeV. The 3-fold difference in body weight loss found between D2 and DBF_1 mice suggests that resistance and susceptibility is a QT amenable to further genetic analysis and mapping (Lander and Kruglyak, 1995). Using information on microsatellite polymorphisms evident between these strains, the author identified chromosomal region that contains the gene(s) that are responsible for strain differences to SeV for the first time.

The analysis revealed a QTL on the distal portion of Chr 4 (*SeV1*), which was significantly linked to post-infection body weight change with an LRS of 14.5, in addition suggestive linkages were also found for QTL on Chr 8 and 14. Furthermore, a highly significant epistatic interaction was detected between *D3Mit182* (SeV2) and *D14Mit10* (*SeV3*, suggestive locus in QTL analysis) at a threshold value of $P < 0.0001$. Taken together the QTL and inter-allelic interaction had explained more than 90% of the genetic effect on disease severity between D2 and B6 mice.

In terms of candidate genes as in many QTL tudy, chromosomal regions significantly influencing the outcome of a disease process are rather large and contain several potential ‘‘candidate genes’’. Although it might be a pure coincidence that the analysis in this study did not allowed us to identify exact genes involved in resistance to SeV, there could be many genes of interest that regulate the function of macrophages and other immune cells as well as cytokines as presented in Table 1.4. The author assessed the most likely genes that could account for three responsible regions, the significant

peak as well as the epistatic interaction. For the *SeV1* region a search between 109 and 132 Mb was performed and identified more than 900 transcripts (RIKEN OmicBrowse, http://omicspace.riken.jp/db/genome.html). Genes were ranked in terms of likelihood based on the amount of evidence extracted during database searches. The search elucidated very strong candidates including the colony stimulating factor 3 receptor (*Csf3r*) and toll-like receptor 12 (*Tlr12*). *Csf3r* functions in neutrophil trafficking and interferon receptor activity. Furthermore, it has been recently reported that neutrophils play a critical role in SeV-induced asthma phenotype (Akk et al., 2008). Mammalian TLRs have been shown to initiate immune responses to infection by recognizing microbial nucleic acids, thereby linking innate and acquired immunity. Recently, it has been reported that two intracellular RNA sensor molecules retinoic-acid-inducible gene I (RIG-I) and Melanoma differentiation-associated gene 5 (MDA5), that recognize RNA viruses, tend to interact with TLRs towards mounting immune response to these viruses (Kato et al., 2006; Strahle et al., 2007; Yount et al., 2008). *SeV2* locus includes interleukin 2 (*Il2*), interleukin 21 (*Il21*), fibroblast growth factor 2 (*Fgf2*), and interleukin 12a (*Il12a*). For the *SeV3* locus, thymic deletion 3 (*Rthyd3*), interleukin 3 receptor alpha chain (*Il3ra*), and interleukin 17 receptor B and D (*Il17rb* and *Il17rd*) are likely candidates. The list of candidates may be even greater than discussed here; however, an interesting aspect of this study is the localization of QTL as well as epistatic interaction influencing the differential response to SeV infection in mice. QTL detected can be fine-mapped in future studies and tested as to whether they represent single or more linked QTL. Regions harboring QTL from one selection line can be made congenic on the opposite line, and phenotype testing of congenic lines can be used to increase the mapping precision and better assessment of the physiological basis of gene function.

Taken together, these observations raise the intriguing possibility that loci controlling basic aspects of resistance and susceptibility to SeV are localized to homologous regions in the genome of other species; hence by exploiting the region of human chromosome showing homologous synteny (*SeV1* for human Chr 1, *SeV2* for human Chr 3, and *SeV3* for mosaic human Chr), prime candidates for resistance and susceptibility to parainfluenza viral infections in humans could be identified, which could further enhance our understanding of the signaling pathway as well as host response to these closely related viruses.

4.5 Summary

Experimental infection of mice with Sendai virus (SeV) is frequently used as a model of viral pathogenesis of human respiratory disease. To understand the differences in host response to SeV among mice strains, the author carried out genetic mapping studies in D2 (susceptible) and B6 (resistant) mice. F1, F2, and N2 backcrossed mice were generated and examined for their disease resistance and susceptibility. For the determination of virulence, percentage body weight loss and survival time were used as phenotypes. A genome wide scan on 108 backcrossed mice for linkage with percentage body weight loss as phenotype was performed. A major QTL showing significant linkage was mapped to the distal portion of Chr 4 (*SeV1*). In addition, two other QTL showing suggestive statistical linkage were also detected on Chr 8 and 14. Furthermore, genome scan was performed for interactions with least square analysis of variance of all pairs of informative makers in backcrossed progenies. A highly significant epistatic interaction between *D3Mit182* and *D14Mit10* was identified, and denoted as *SeV2* and *SeV3*, respectively, and the latter was the same locus showing a suggestive level on Chr 14 in QTL analysis. Considered genotypes of these three loci, could account for more than 90% of genetic effect on the differential response to SeV infection between B6 and D2 mice. These findings revealed a novel gene interactions controlling SeV resistance in mice and will enable the identification of resistance genes encoded within these loci.

5.0 PART 2

5.0 Transcriptome profile characterizing pathogenesis of host response to Sendai virus infection in mice

5.1. Introduction

Respiratory paramyxoviral infections are leading cause of serious respiratory disease in humans especially among children. The severity varies from non-clinical or mild upper respiratory tract infections to severe lower respiratory tract infections that may lead to hospitalization and sometimes death (Chanock, 2001). In addition, there are reports that respiratory viral infections vary in clinical presentations with associated altered cytokine profiles and high viral load (Laham et al., 2004; de Jong et al., 2006; Faisca and Desmecht, 2007; Melendi et al., 2007). Moreover, immune therapies for this kind of illness are very limited; this limitation is due to at least in part to our incomplete understanding of the genetic basis of the differential immune response to respiratory viruses. Sendai virus (SeV) which is thought to be a natural respiratory pathogen of mice was shown to display a wide spectrum of resistance and susceptibility among mice strains (Itoh et al., 1989; Faisca et al., 2005). However, the variation in sensitivity to SeV was not only because of genetic restriction of viral infection and replication rather was the result of some aberrations or differences in the humoral or cell-mediated immune response. In addition, evidence has been accumulating that children with severe respiratory infection suffer from enhanced inflammatory lesions caused by cytokine storm, rather than virus induced cytopathology (Gern et al., 2006, Melendi et al., 2007). SeV resistant mice are known to repress initial viral replication, restrict viral spread and airway pathology, and finally eliminate the virus, while susceptible mice tend to allow viral replication and spread with severe pathological outcomes (Itoh et al., 1991; Faisca and

Desmecht, 2007). This suggests that host immune response might be playing a crucial role in severity of respiratory viral infections caused by these closely related viruses. The innate immune system represents the evolutionary ancient part of vertebrate immunity and relies on germ line encoded receptors commonly referred to as pattern recognition receptors, to mediate immune responses to pathogenic microorganisms (Medzhitov, 2001; Kawai and Akira, 2006). Triggering of these receptors activates a variety of signal transduction pathways ultimately resulting in large alterations of the host transcriptome profile, of which the dynamic complexity and underlying mechanisms are poorly understood, especially at the whole organism level. SeV has been known to be an excellent inducer of IFN as well as other cytokines such as IL-2, TNF, IL-6 and IL-10 (Mo et al., 1995). Although primary SeV infection induces both Th1 and Th2 responses with the production of inflammatory cytokines (Mo et al., 1997a), however, IL-4 (Mo et al., 1997b), *Tlr4* (van der Sluijs et al., 2003) and *Tlr3* (Elco et al., 2005) were shown not to interfere with SeV infection. Animal models of viral respiratory disease have similar traits to human respiratory infections and can be used to investigate the mechanism associated with disease severity. In addition, transcriptional profiling has provided a great amount of information about host pathogen interactions. Most of these studies monitored changes in gene expression in the host cells after contact with specific pathogen *in vitro*. While these studies can provide information concerning cell-autonomous differences in the response to infection, *in vivo* analyses are required to detect differences in the complex multifactorial interactions between the pathogen and host in a real infection, especially in the coordinated behavior of the host immune system. Furthermore, the comparison of the microarray data for acute lung inflammation models from 12 studies (exposures to air pollutants; bacterial, viral, and parasitic infections; and allergic asthma models), of which the cluster includes

subsets such as inflammatory response, IFN-induced genes, immune signaling, or cell proliferation, of these subsets, the inflammatory response was common to all models. However, IFN-induced responses were more pronounced in viral models. In addition, responses to influenza in macaques were weaker than in mice, reflecting differences in the degree of lung inflammation and/or virus replication (Pennings et al., 2008). Thus, the author hypothesized that there could be differences in the expression of inflammatory cytokine/chemokine and their receptor genes among murine strains after SeV infection. Taken together, in this study, the author compared and determines the differences in the kinetics of cellular influx, viral replication, pathogenesis and transcriptional immune signatures of an airway inflammatory response between resistant B6 and susceptible D2 mice strains, which represents two polar extremes of response to SeV induced pneumonia. The results provided a global view of the differential early and late changes in immune response to SeV infection, from which the author was able to extract components pointing to possible mechanisms accounting for the genetic differences in susceptibility and also provided clues to the respiratory viral pathologies seen in children. Furthermore, the identification of immune regulatory factors involved in the interaction of SeV with these hosts, will provide deeper understanding of beneficial or detrimental pulmonary immune mechanisms, which will lead to the development of new strategies for the control human respiratory viral infections.

5.2. Materials and Methods

5.2.1. *Animals*

Eight weeks-old SPF female 57BL6/J (B6) and DBA2/J (D2) mice were purchased from Japan SLC (Shizuoka, Japan), and used for all experimental procedures under SPF conditions. Mice from each strain were divided into four groups, for sampling on day 2, 4, 8 and 14 post infection (p.i); same aged mice were used as controls. For sampling at indicated time points; mice were sacrificed with the intra-peritoneal injection of pentobarbital sodium (Somnopentyl, Schering-Plough Animal Health, NJ, USA) and followed by cervical dislocation. The Institutional Animal Care and Use committee of Hokkaido University approved all experimental protocols.

5.2.2. *Virus and infection*

The MN strain of SeV was kind gift from Prof. Hiroshi Iwai, Rakuno Gakuen University. Seed virus stock in modified Eagle medium (Sigma, MO,USA) with 1% bovine serum albumin was inoculated into 10-day-old embryonated chicken eggs and incubated for 72 h at 35ºC. After allantoic fluid recovered from inoculated eggs was centrifuged at 2,500 x g for 20 min, the supernatant was collected and stored at -80 ºC until used for infection to mice. Virus titer in the allantioc fluid was determined by hemadsorption assay using a monkey kidney cell line, LLC-MK2, and chicken red blood cells. The values of virus titer were indicated as median tissue culture infectious dose ($TCID_{50}$). Mice were infected with median tissue culture infectious dose (10^3 $TCID_{50}$) of SeV in Medium 199 (Sigma, MO, USA). A volume of 25 µl of the viral innoculum was slowly instilled intranasally, following anesthetization with intra-peritoneal injection of pentobartital sodium. Generally, for the determination of virulence, a representative of infected mice and that of control were weighed daily and monitored by

visual inspection twice per day, with the main visual disease signs being lethargic, ruffled fur, hunching, and dyspnea.

5.2.3. *Pulmonary lavage cytology*

Four mice from each group of B6, D2 and that of the control mice were sacrificed at indicated time points and bronchoalveolar lavage fluid (BALF) samples were collected by exposing the trachea with a midline incision, left main stem bronchus was isolated, clamped, and the trachea cannulated with a sterile 22-gauge Abbocath-T catheter. The right lung lobes were lavaged five times with warm Hanks balanced saline solution (HBSS pH 7.2, body weight × 35 ml/kg 37°C). BALF was centrifuged at 800 × g for 10 min and the supernates were stored for cytokine analysis (−80°C). BALF cells were resuspended in 1,000 μl Dulbecco's minimal essential medium (DMEM) containing 10% fetal bovine serum (FBS), and total number of cells was determined with a hemacytometer. Additionally, 200 μl of resuspended cells were adhered in duplicate onto glass slides using a Cytospin (Cytospin 3 centrifuge, Shandon, Pittsburgh, PA) and subsequently stained with Giemsa solution (Merck KGaA, Darmstadt, Germany) for cell differentiation determination, with at least 300 cells counted from each slide and was used to calculate the percentages of various cells for each group of mice. Results were expressed as mean ± SE values for each group

5.2.4. *Determination of viral titers in lungs of Sendai virus infected mic*e

To determine viral titers of all mice groups total RNAs were obtained from the homogenized lungs tissues of all mice groups at indicated time points using TRIzol reagent (Invitrogen, Carlsbad, CA, USA). The purified RNAs were treated with DNase for DNA digestion (Nippon Gene, Toyama, Japan) and synthesized to cDNAs using ReverTra Ace (Toyobo, Osaka, Japan) and Oligo dT Primer (Invitrogen,

Carlsbad, CA, USA). A two-step quantitative real-time PCR analysis was performed using the Brilliant SYBR Green QPCR Master Mix and the real-time thermal cycler (MX 3000; Stratagene, Milano, Italy). The amplification conditions were as follows: 10 min at 95ºC, 40 cycles of 10 s at 95ºC, 20 s at 58ºC, and 20 s at 72ºC, 1 cycle of 10 s at 95ºC, 20 s at 58ºC, and 20 s at 95ºC. ROX dye was included in each reaction to normalize non-PCR-related fluctuations in the fluorescence signals. The amplification specificity of all the PCR reactions was confirmed by melting curve analysis. No-template controls were included for each primer pair to assess any significant levels of contaminants. Relative quantification of the SeV mRNA copies of the gene was normalized to the expression of *β-actin* (Table 1.5). The viral load present in a sample was calculated using standard curve of particle counted SeV included in the assay run, and Student's *t*-test was used to analyze the differences in lung virus titers between the groups of mice following natural log-transformation of the data.

5.2.5. *Lung histopathology analysis of Sendai virus infected mice*

Lungs were flushed with sterile saline removed from all mice groups at indicated time points after SeV infection and fixed in acetate-buffered 4% formaldehyde solution and, after 24 h, washed with sterile saline, re-suspended with 70% ethanol, and stored at 4°C until processed. Lungs were embedded in paraffin and sections were cut 5-µm thick in duplicates, stained with hematoxylin–eosin, and examined under the light microscope. The degree of distribution and severity of inflammatory infiltrates/structural alterations were examined around small airways and adjacent blood vessels, changes were graded on a scale of 1–6 (1: Normal; 1: slight/ mild; 2: moderately severe; 4 and severe/high; 6). The pathology scores for lung sections were averaged and summarized as pathological index. Values were expressed as mean ± SE values for each group.

5.2.6. *Bronchoalveolar lavage fluid (BALF) cytokine analysis*

Following infection with SeV, collected BALF was analyzed for the expression levels of mouse inflammatory cytokines; IL-1A, IL-1B, IL-2, IL-4, IL-6, IL-10, IL-12, IL-17A, IFN-γ, TNF-α, granulocyte colony-stimulating factor (G-CSF) and granulocyte-macrophage colony-stimulating factor (GM-CSF) in lavage fluid were determined using Multi-Analyte ELISArray Kit profiler (SABiosciences MD, USA. catalog no #MEM-004A). The kit analyzes the concentrations of these proteins as well as set of standard negative and positive controls also included in the kit. For testing of BALF cytokine profile 50 µl of each sample from all groups of mice at indicated time points was analyzed in duplicates and concentrations of cytokines was determined by comparing the standard positive and negative controls at 450 nm. Data were obtained using the SoftMax Pro version 5 software program (MDS Analytical Technologies, Ontario, Canada) for standardization and standard curve acquisition followed by conversion to Excel format (Microsoft Corporation, Seattle, WA) for further analysis. Comparisons of BALF cytokine measurements were made with Mann-Whitney test, *P*-value less than 0.05 was considered significant and data were analyzed with SPSS 16.0 (Chicago, IL)

5.2.7 *RNA isolation and RT^2 Profiler PCR Array*

Total RNA was isolated from lung tissues of all infected mice groups and that of the control at indicated time points using TRIzol reagent (Invitrogen, Carlsbad, CA, USA). RNA samples were refined using an RNeasy Micro Kit (Qiagen, Germantown, MD) and treated with Turbo-free DNase (Ambion) for DNA digestion and elimination. Thereafter it was re-cleaned again. One microgram of each total RNA sample was converted into first-strand cDNA using RT^2 PCR Array First Strand Kit (SABiosciences, Frederick, MD USA). Each RT^2 Profiler PCR Array was performed in duplicate on a

96-well format using 10 µl of cDNA targeting the mRNA levels of the 84 Mouse Inflammatory Cytokines/Chenokines and Receptors, (SuperArray Bioscience Corporation; catalog no #PAMM-011-12A). The genes list were; chemokine genes (*Ccl1, Ccl2, Ccl3, Ccl4, Ccl5, Ccl6, Ccl7, Ccl8, Ccl9, Ccl11, Ccl12, Ccl17, Ccl19, Ccl20, Ccl22, Ccl24, Ccl25, Cx3cl1 (Scye1), Cxcl1, Cxcl4, Cxcl5, Cxcl9, Cxcl10, Cxcl11, Cxcl12 (Sdf1), Cxcl13, Cxcl15*), chemokine receptors (*Ccr1, Ccr2, Ccr3, Ccr4, Ccr5, Ccr6, Ccr7, Ccr8, Ccr9, Cxcr3, Il8rb, Xcr1*), cytokine genes (*Ifng, Il1a, Il1b, Il1f6, Il1f8, Il3, Il4, Il10, Il11, Il13, Il15, Il16, Il17b, Il18, Il20, Itgam, Itgb2, Lta, Ltb, Mif, Spp1, Tgfb1, Tnfa, Cd40lg*), and cytokine receptors (*Ifngr1, Il1r1, Il1r2, Il2rb, Il2rg, Il5ra, Il6ra, Il6st, Il8rb, Il10ra, Il10rb, Il13ra1, Tnfrsf1a, Tnfrsf1b*), and other genes involved in inflammatory response (*Abcf1, Bcl6, Blr1, C3, Casp1, Crp, Tollip*). The quantitative RT^2-PCR array was run on an MX 300 thermal cycler (Stratagene, La Jolla, CA). The PCR array mix was denatured at 95°C for 10 min before the first PCR cycle. The thermal cycle profile consists of denaturation for 15 s at 95°C and annealing for 60 s at 60°C. A total of 40 PCR cycles were performed. Data analysis was performed using the manufacturer's integrated web-based software package for the RT^2 PCR Array System using ΔΔCt based fold-change calculations. The expression levels of each mRNA were normalized using the expression of *Gusb, Hprt1, Hsp90ab1, Gapdh*, and *Actb,* considered the housekeeping genes. Changes in gene expression were analyzed by *t*-test with the use of appropriate cutoff criteria, a 10-fold induction or repression of expression, with a *P* value of <0.05, was considered to represent significantly up- or down-regulated gene expression. The author further characterized the gene expression response patterns in B6, D2 and control mice by carrying out gene cluster analysis of indicated time points, which created a 2D gene tree using an average linkage clustering heat map method (SuperArray RT^2 PCR Array Data Analysis Web-base Software). The

dendrogram illustrates the hierarchical time points of the lung of each mice group, and an average cut off for gene changes in fold expression was considered to be significant at $P < 0.001$.

5.2.8 *Validation of gene expression by Two-step real-time quantitative PCR*

In addition to RT^2 Profiler PCR Array analysis four genes were selected and their expression levels were measured by two-step Quantitative real time PCR and *β-actin* was used as internal control. The following genes were use: NM_008350 (*Il11*), NM_019508 (*Il17b*), NM_009263 (*Spp1*) NM_011577 (*Tgfb1*) and NM_007393 (*β-actin*) (Table 1.5). To examine their mRNA expression, total RNAs were obtained from the lungs of all mice groups at indicated time points using TRIzol reagent (Invitrogen, Carlsbad, CA, USA). The purified RNAs were treated with DNase for DNA digestion (Nippon Gene, Toyama, Japan) and synthesized to cDNAs using ReverTra Ace (Toyobo, Osaka, Japan) and Oligo dT Primer (Invitrogen, Carlsbad, CA, USA). The quantitative real-time PCR analysis was performed using the Brilliant SYBR Green QPCR Master Mix and the real-time thermal cycler (MX 3000; Stratagene, Milano, Italy) to obtain cDNAs. The amplification conditions were as follows: 10 min at 95ºC, followed by 40 cycles of 10 s at 95ºC, 20 s at 58ºC, and 20 s at 72ºC, 1 cycle of 10 s at 95ºC, 20 s at 58ºC, and 20 s at 95ºC. ROX dye was included in each reaction to normalize non-PCR-related fluctuations in the fluorescence signals. The amplification specificity of all the PCR reactions was confirmed by melting curve analysis. No-template controls were included for each primer pair to assess any significant levels of contaminants. Relative quantification of the mRNA copies of all genes was normalized to the expression of *β-actin*. The ratio of genes was calculated from these normalized values and expressed as fold change compared to those of controls.

5.3 Results

5.3.1 *Induction of Sendai virus pneumonia and kinetics of pulmonary response*

As the first step towards characterizing the differential host defense against respiratory SeV infection, groups of B6 and D2 mice were inoculated by intra nasally with 1×10^3 $TCID_{50}$ on day 0 and their clinical signs were monitored. Intranasal infection with 1×10^3 $TCID_{50}$ of SeV resulted in a transient weight loss reaching a nadir between 7-8 days after infection in both B6 and D2 mice (Fig 1.8 A; $P < 0.05$ compared to control). However, D2 mice tend to loose more weight as compared to B6 mice, and with the later recovering and returning to normal weight levels by day 14, thereby maintaining its normal appearance. While in all occasions D2 mice, showed severe susceptibility to the virus, with severe clinical signs and fail to recover thereby terminating to death between 9-10 days as the usual end points.

To elucidate the mechanism of the differential sensitivity to SeV-induced pneumonia in these mice, the kinetics of pulmonary recruitment of inflammatory cells in response to the infection was determined. Inflammatory cellular influx in infected mice emerges by day 2 after SeV infection; however, the total cellular population and their composition in BALF of both mice strains did not change considerably, which mainly consisted of macrophages and very few neutrophils as compared with the control (Fig 1.8 B). On the other hand, on day 4, total leukocytes count in BALF increased approximately 5 and 9-fold in B6 ($*P < 0.05$) and D2 ($***P < 0.001$) mice, respectively, compared with that of the control mice. In addition, D2 mice had 2-fold cellular influx than B6 ($**P < 0.05$) consisting of mainly macrophages, neutrophils, and lymphocytes. D2 mice continued to have higher number of cellular infiltration up to day 8 as compared to B6 mice and by day 14 cellular influx in B6 declined to

almost the same level as compared to that of the controls. The author postulated that the differential pulmonary cellular infiltrations seen in these mice might be attributed in part to transcriptional regulation of immune mediators or the rapid destruction of immune and endothelial cells as a result of viral replication, which could possibly account for their differential susceptibilities. Therefore, viral titers from lung tissues of the two strains and that of the control mice at 2, 4, 8 and 14 days after infection were determined (Fig. 1.8 C). From 2 to 8 days after infection, viral titers increased significantly and peaked on day 4 in both mice strains when compared to the controls (Control vs B6 $**P < 0.005$; Control vs D2 $***P < 0.0001$). Following determination, the viral load increased significantly in D2 mice ($*P < 0.05$) as compared to B6 mice, which had only a considerable increase on day 4 and by day 8, viral titers become very low which coincided with the time of viral clearance and cumulated to undetectable level by day 14. This finding, was consistent with previous reports of viral clearance between 12-21 days after SeV infection which were determined by end point titration in embryonated eggs (Hou et al., 1992; Zhong et al., 2001). It should be noted that viral load was measured by real time quantitative RT-PCR instead of standard plaque assay. These methods may differ in their outcome, since standard plaque assay only detects viable virus (i.e virus that been shed by infected cells), whereas molecular techniques detect all viral genomes. Although these methods of analysis differ from other reports (Brownstein and Winkler, 1986; Itoh et al., 1991), the present analysis reconfirms previous report, that there are indeed differences in viral loads amongst resistant and susceptible mice strains (Faisca et al., 2005). The viral titers in D2 mice correlate with severity of the disease and it clearly shows that these mice lack the capacity to clear the virus. Conversely, these results suggest that there is indeed a connection between the pulmonary titers and the morphological and clinical characteristics of the infection.

5.3.2 *Lung histopathology changes in response to Sendai virus induced pneumonia*

Consequently, the previous data suggest that the two mice strains differ in their response to SeV induced pneumonia; therefore, the author investigated differences in inflammation and compared lung histopathological changes at indicated time points in these mice strains after viral infection. Lungs from SeV-infected B6, D2 and that of the control mice were harvested on days 2, 4, 8 and 14 and examined grossly. Incidence of lung consolidation was much more severe in D2 as compared to B6 mice. Thereafter harvested lungs were sectioned and stained with hematoxylin-eosin. The lungs were examined and graded microscopically using a pathological index. Figure 1.9A shows the representative sections and taken at indicated time points from each group of mice at low and high power to demonstrate the relative amount of pathological changes that developed in the lung of each strain. Histopathological lung lesions developed in the two mice strains, but the degree of the lesions is much more severe in D2 than in B6 mice. There was little difference between the first histological profile of B6 mice and normal morphology of murine lungs on day 2. The airways did not contain exudates and the epithelium appeared generally intact. On days 4 and 8, the cell density in interstitium appeared slightly elevated; however, this returned to normal level by day 14. The histological diagnosis most compatible with these observations was slight broncho-bronchiolitis. In contrast, D2 mice had exudates in the alveolar spaces contain mixtures of cell debris epithelial cells, neutrophils, lymphocytes and morphologically altered macrophages (cytoplasmic vacuolation, pycnosis, karyorhexis). From day 4 to 8, the epithelial lining exhibited large areas of deciliation alternating with degeneration, necrosis, desquamation and marked hyperplasia with uneven thickness and cell arrangements. The lamina propria was infiltrated multifocally by numerous macrophages, neutrophils and lymphoid cells with

round nuclei which generated the characteristic perivascular cuffing, and this was diagnosed as severe necrotizing and purulent broncho-broncholitis with multifocal alveolitis (Figure 1.9 A and B).

5.3.3 *Proinflammatory BALF cytokine response to Sendai virus induced pneumonia*

The cellular inflammatory influx and histopathological changes suggest that these two mice strains might differ in their immune response to SeV infection. To determine whether an altered proinflammatory cytokine response could account for the observed differential response to SeV infection, the virus-induced cellular pulmonary cytokine responses of B6, D2 and control mice were investigated. The cellular pulmonary cytokine protein levels of BALF from these mice was compared, of which the panel consist of some the cytokines implicated previously in the pathogenesis of respiratory SeV infection, which were determined over the course of the infection responses (Mo et al., 1995; Mo et al., 1997a; Mo et al., 1997b). The inflammatory cytokines include IL-1α, IL-1ß, IL-2, IL-4, IL-6, IL-10, IL-12, IL-17α, IFN-γ, TNF-α, G-CSF and GM-CSF. SeV infection seems to induce most of these BALF cytokine levels in both strains of mice with the majority of the assayed cytokine reaching their peak levels on day 4 or 8 p.i as compared to control mice (Fig 2.0). On day 2 p.i, we observed the induction of some of the cytokines; however, D2 mice had a significantly higher levels of IL-6 and IFN-γ (P<0.05) as compared to B6 mice (Fig 2.0), indicating the immediate and early response to viral induced stress in D2 mice. Interestingly on day 4 p.i, a very distinct and robust response to SeV-induced pneumonia in both mice strains was observed, with D2 mice producing a much higher amount of cytokines as compared to B6 mice, which correlates with the amount of cellular influx in this strain. The response in D2 mice were driven by significant levels of IL-1ß, IL-2, IL-6, and TNF-α as compared to B6 (P < 0.05), with very high levels of IFN-γ and GM-CSF which was consider as a Th1-mediated

response. While the response in B6 mice was mediated by significant levels of IL-1α, IL-4, IL-10, IL-12, G-CSF ($P < 0.05$) and with moderate levels of IL-6 and GM-CSF, which was denoted as Th1/Th2-mediated response, and coincides with high influx of inflammatory cells in both mice strains compared to the controls. Furthermore, day 8 p.i response was very distinct between the two strains, which coincided with the time of viral clearance in B6 and severe pathology with persistent high viral titer observed in D2 mice. The levels of these cytokines (IL-1ß, IL-2, IL-6, IFN-γ, TNF-α, GM-CSF) remained steadily and significantly high in D2 mice ($P < 0.05$), in contrast with B6 mice, which had a reduction in the levels of the cytokines with significant levels of IL-10 and IL-12 ($P < 0.05$). Furthermore, BALF in B6 and control mice on day 14 p.i was analyzed and compared; except for IL-6 and IL-12 , other cytokines returned to normal baseline levels, thus coincides with the time for the viral titer becomes undetectable and tissue regeneration and remodeling had taken place in this strain (Fig 1.8 C, Fig 1.9 A). Taken together, D2 mice tend to respond early to SeV infectionm while B6 mice maintained a balance between Th1-and Th2-mediated response, thereby mounting an effective immune response in a well-coordinated fashion. Thus, the clearly defined pathophysiological and proinflammatory BALF cytokine differences in these strains points to the fact that there could be host genetic immune transcriptional variation that are responsible for the differential immune responses. Therefore, the author sought to define further the host transcriptional immune responses that might mediate differential susceptibility to SeV-induced pneumonia in these two mice strains.

5.3.4 *Transcriptional immune gene regulation in lung upon Sendai virus induced pneumonia*

Thus, the initial results indicate that B6 has a conferred genetic molecular mechanism of abrogating the infection, while D2 mice succumbed to the infection. In addition, the mortality usually

exhibited by D2 mice occurs during the timeframe of when a virus-specific adaptive immune response would develop. To gain insight into the observed differential response, the author assessed the inflammatory cytokines/chemokines and receptors genes that are likely to be induced at early and late time points after SeV infection in these two mice strains. Therefore, a comparative transcriptional profiles of the lungs of SeV-infected B6, D2 and control mice on days 2, 4, 8 and 14 after SeV inoculation were performed using quantitative RT-PCR analysis of an array of 84 inflammatory cytokines and chemokines and their receptors (n = 4 per group at indicated time points, equal amounts of total RNA from all mice groups were pooled). Cluster analysis of all arrays clearly shows that the two mice strains infected with SeV showed a distinct pattern of responses to SeV-induced pneumonia through out the course of infection, and all genes in both mice strains showed altered differential expressions as compared to controls (Fig 2.1). Two days post infection, D2 mice mounted an early immune response to SeV infection with the immediate up-regulation of genes for some key cytokines/chemokines and receptors which include, *Ifng, Tnfrsf1a*, *Tnfrsf1b*, *Il2r*b, *Il3*, *Il5r*a, *Il11*, *Scye1*, *Ccl3*, *Ccl11*, *Ccl19*, *Ccl22*, *Ccl25* and *Cxcl1*, and other related inflammatory genes such as *Abcf1* and *C3* when compared to B6 which had only the induction of *Il6ra*. Furthermore, on day 4 p.i, which coincided with the time of viral replication and activation of the immune response, the set of genes up-regulated in B6 are either down-regulated or distinct as compared to D2 mice, confirming the differential transcriptional immune response to SeV infection between these two strains. These data closely parallel the cellular influx, viral titers and proinflammatory cytokine response observed at 4-day p.i (Fig 1.8 B, C, D and Fig 2.0). Conversely, D2 mice tend to show a consistent pattern of up and down-regulated genes through out the course of infection, whereas in B6, the strongest response was detected on day 4 p.i with the

up-regulation of most of the cytokines/chemokines receptors genes and thereafter they fade away or remained at undetectable level on day 8 p.i, and with only a few set of genes that were up-regulated (*Il1r2*, *Cxcl13*, *Cxcr3*, *Ccl5*, *Ccr2*, *Itgam, Cxcl15*, *Cxcl10*, *Il6st*, *Il1b*) in this strain. These suggested the ability of B6 to repress SeV infection and parallel the decrease in viral titer and less severe lung pathology seen in this strain, and also indicated the coordinated behavior of B6 immune system in combating the SeV-induced pneumonia. On day 8-p.i, D2 mice showed a slight deviation from consistently up-regulated genes (day 2-4) with new set of genes being activated in this strain, which shows its inability to mount an effective immune response and also relates to the persistent steady level of high viral titers and severity of lung pathology observed, and correlates to high degree of altered host genes immune regulation. Next, the author compared day 14 p.i controls and B6 mice and found out that only few genes showed altered regulation in the later, which corresponds to the complete elimination of viral particles and remodeling of lung architecture, therefore agreeing with earlier reports of SeV infection in resistant strains characterized by slight peak of viral titers on fourth to fifth day, thereafter virus titer declines rapidly with post infectious virus no longer detectable after the 10th -11th day p.i.

Taken together, this analysis revealed that B6 mice tend to produce lower amount of proinflammatory cytokines/chemokines and effectively clear the virus, while D2 mice succumbed after infection had high viral loads and increased production of proinflammatory cytokines/chemokines early after infection, which becomes detrimental to the host. Therefore, the author sought to identify the underlying mechanism responsible for this difference, and carried out a detailed comparative analysis of consistently up and down- regulated proinflammatory cytokine/chemokine genes in D2 compared to B6 mice of all indicated time points. Log2 *t*-test* fold-changes was used for the analysis in genes

expression with a cut off criteria of 10-fold up or down regulation were considered significant at $P < 0.05$ based on reliable Ct-values. Fifty six genes exhibiting differential relative levels of expression in D2 as compared to B6 mice were detected. In addition, the analysis further revealed 26 and 5 significantly up-and down-regulated genes, respectively, out of the 56 genes showing relative levels of expression ($P<0.05$) (Table 1.6). The consistently up-regulated genes for cytokines/chemokines and receptors in D2 mice were dominated by chemokine CC family (*Ccl3* (MIP-1A), *Ccl11 Ccl19*, *Ccl22*), interleukins (*Ifng*, *Il3*, *Il11*, *Il13*, *Il16*, *Cx3cl1*(*Scye1*)), chemokine CXC family (*Cxcl1*, *Cxcl10* (IP-10)), chemokine receptors (*Ccr8*, *Ccr9*, *Xcr1*), cytokine receptors (*Il2rb*, *Il5ra*, *Il6st*, *Tnfrsf1a*, *Tnfrsf1b*) and other inflammatory related genes (*Abcf1*, *C3*, *Crp*, *Tollip*), with the down regulated genes which includes *Ccl5* (RANTES), *Itgam*, *Ltb*, *Spp1* and *Tgfb1*. Previously, some of these genes have been reported to be inducible by SeV; *Ccl3*, *Cxcl10*, *Ifng* and *Il13* (Matikainen et al., 2000; Cai and Castleman 2002; Elco et al., 2005; Kohlmeier et al., 2008) and they have been incriminated in the immunopathology of the disease. Based on these findings that B6 mice are able to repressed viral replication and effectively clear the virus with less severe pathological outcomes. The author decided to look closely the set of genes that were regulated on day 4 p.i. The response in B6 were modulated by sets of up-regulated genes based on functional groupings which includes; chemokine genes (*Ccl2*, *Ccl4*, *Ccl6*, *Ccl7*, *Ccl8*, *Ccl9*, *Ccl12*, *Ccl17*, *Ccl24*, *Cxcl4*, *Cxcl5*, *Cxcl9*, *Cx3cl1*), chemokine receptors (*Ccr3*, *Ccr4*, *Ccr5*, *Ccr6*, *Ccr7*, *Ccr10*, *Cxcr5*), cytokine genes (*Il1A*, *Il1f8*, *Il1f6*, *Il4*, *Il10*, *IL20*, *Tnf*, *Lta*, *Ltb*, *Cd401g*, *Tgbf1*, *Itgam*), cytokine receptors (*Il1r1*, *Il2rg*, *Il8rb*) and other inflammatory response genes (*Casp1*) (Fig 2.1). Consistent with these findings, *Ccr5*, *Ccl5*, *Ccl7*, *Il4*, *Il10* and *Tnf*, (Itoh et al., 89; Mo et al., 1997a; Grayson et al., 2007) had been reported to be involved in SeV immune response. The expression of genes for some cytokines

such as *Tnf*, *Tgbf1*, *Il10* and *Il11* in B6 which has been known to act in part immunosuppressively or by specifically targeting pathogens, indicates equally and important aspect of the immune response, as these genes will help restore the host cell to its normal state when the inflammatory stimulus is no longer present, thus keeping the system in check, whereas these genes in D2 mice might cause the exacerbation of the disease process. Next, of all the total number of genes analyzed in this study, some of set of genes that includes *Ifng*, *Itgb2*, *Il1B*, *Il3*, *Il10rb*, *Il11*, *Il18*, *Ccl20*, *Ccl25*, *Cxcl1*, *Cx3cl*, *Abfcf1* and *Bc16* were commonly up-regulated in both mice strains (Fig 2.1). Although, the two strains showed a clearly distinct response to SeV-induced pneumonia, there exists a pathway that they could be exerting similar immune response. However, the expression of inflammatory mediators triggered by SeV infection was distinct in terms of absolute values, phases and tissue damage, depending on the mouse strain. These differences can be associated to the severity and progression of the disease, which might results in death of the susceptible D2 strain, and in the disease control in the resistant B6 strain.

5.3.5 *Validation of potential differentially expressed genes in lungs of infected mice by quantitative real-time PCR*

To validate and confirm the gene expression changes found by RT-PCR array analysis, primers were designed and quantitative real-time PCR was performed. For this purpose, two genes that displayed relatively up-regulation were selected; *Il11* (>4.26 fold up-regulation, P<0.05) and *Il17b* (>2.58 fold up-regulation, $P < 0.05$), and two other genes which were down regulated in D2 mice but up-regulated in B6; *Spp1* (< -7.06 fold down regulation, $P < 0.000$) and *Tgfb1* (< -5.78 fold down regulation, $P < 0.003$) were also selected (Table 1.6 and Fig 2.1). The two genes that were up-regulated in both stains which were detected using RT-PCR profiling were also up-regulated using quantitative

real-time PCR (Fig 2.2). In addition, two genes which were down-regulated in D2 mice but up-regulated in B6 showed similar phenomenon, indeed this confirms the consistency and accuracy of the RT-PCR array profiling.

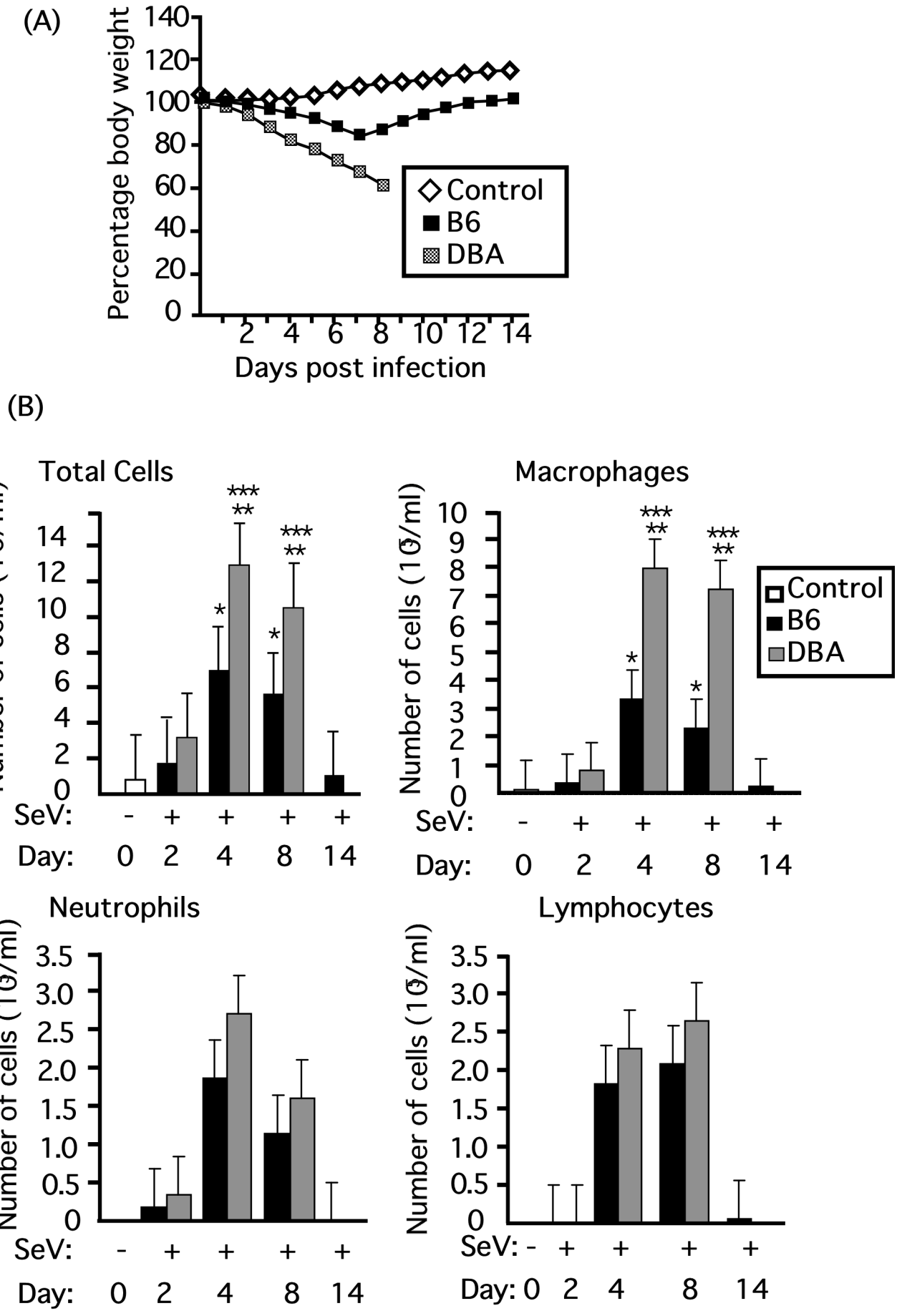
(A)
Percentage body weight
140
120
100
80
60
40
20
0
2 4 6 8 10 12 14
Days post infection
Control
B6
DBA
(B)
Total Cells
Macrophages
Neutrophils
Lymphocytes
Number of cells (10⁵/ml)
SeV: - + + + +
Day: 0 2 4 8 14
Control
B6
DBA

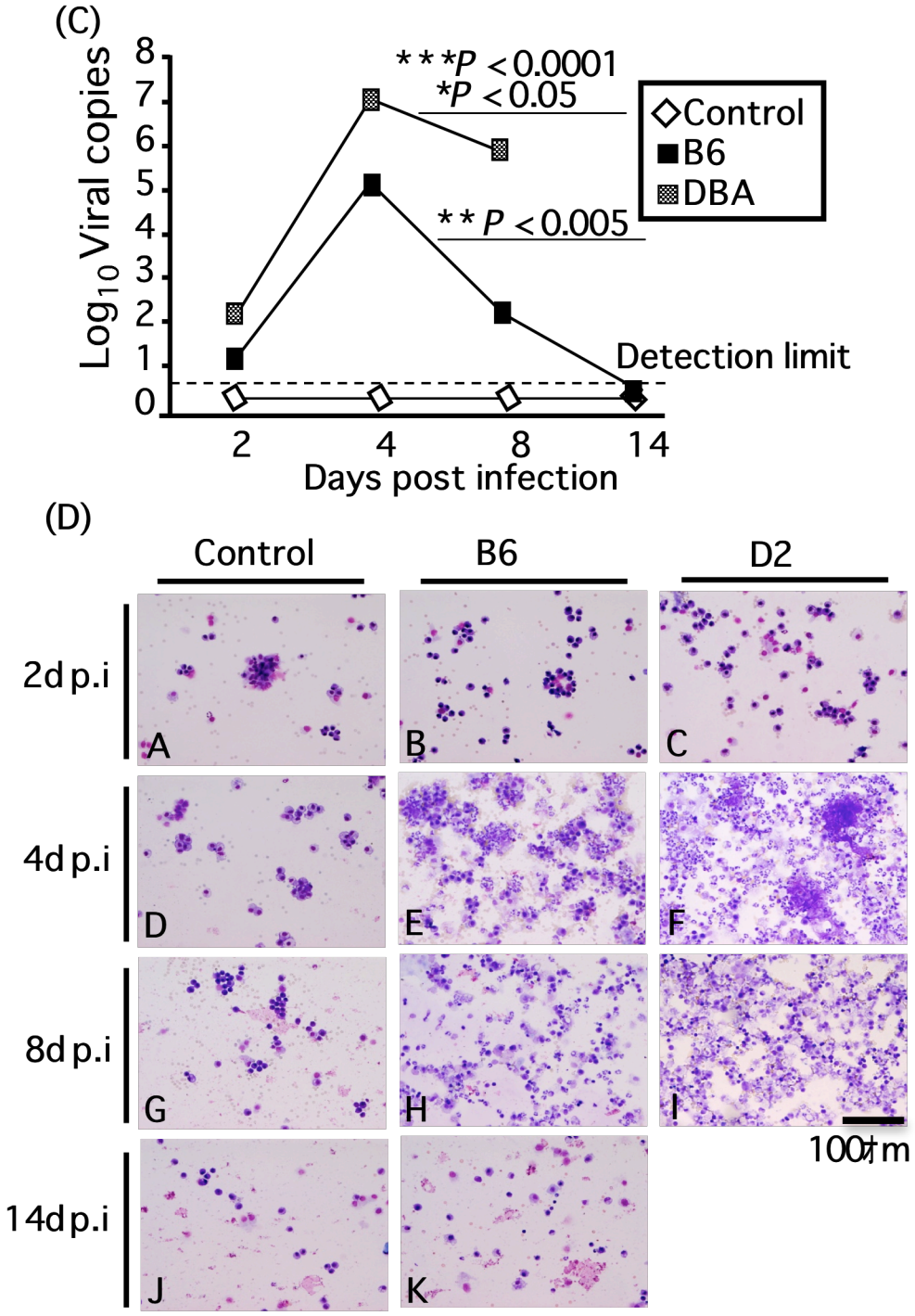

Fig 1.8. Body weight changes in B6 (black squares), D2 (grey squares) and control (open triangles) same aged mice (A), after inoculation with SeV on day 0 and monitored for 14 days; (B) The total cellular composition and diferential counts in the bronchoalveolar lavage fluid from groups of four B6 (black bars), D2 (grey bars) and control (open bars) mice following inoculation with SeV, on days 2, 4, 8 and 14, mice were exsanguinated, their lungs were lavaged. Total cell counts on both day 4 and 8 p.i $*P < 0.05$ Control vs B6; $***P < 0.001$ Control vs D2 and $**P < 0.05$ B6 vs D2. Data are presented as mean total leucocytes and mean absolute values of differential counts (Macrophages, Neutrophils and lymphocytes) ± SEM. (C) qRT-PCR analysis of lung viral titers after infection with SeV and titers are expressed in log10 viral copies, $***P < 0.0001$ Control vs D2; $**P < 0.005$ Control vs B6 and $*P < 0.05$ D2 vs B6. (D) Photomicrograph representation of pulmonary cellular influx from BALF of all mice groups at indicated time points; Giemsa staining, Bar = 100 μ m.

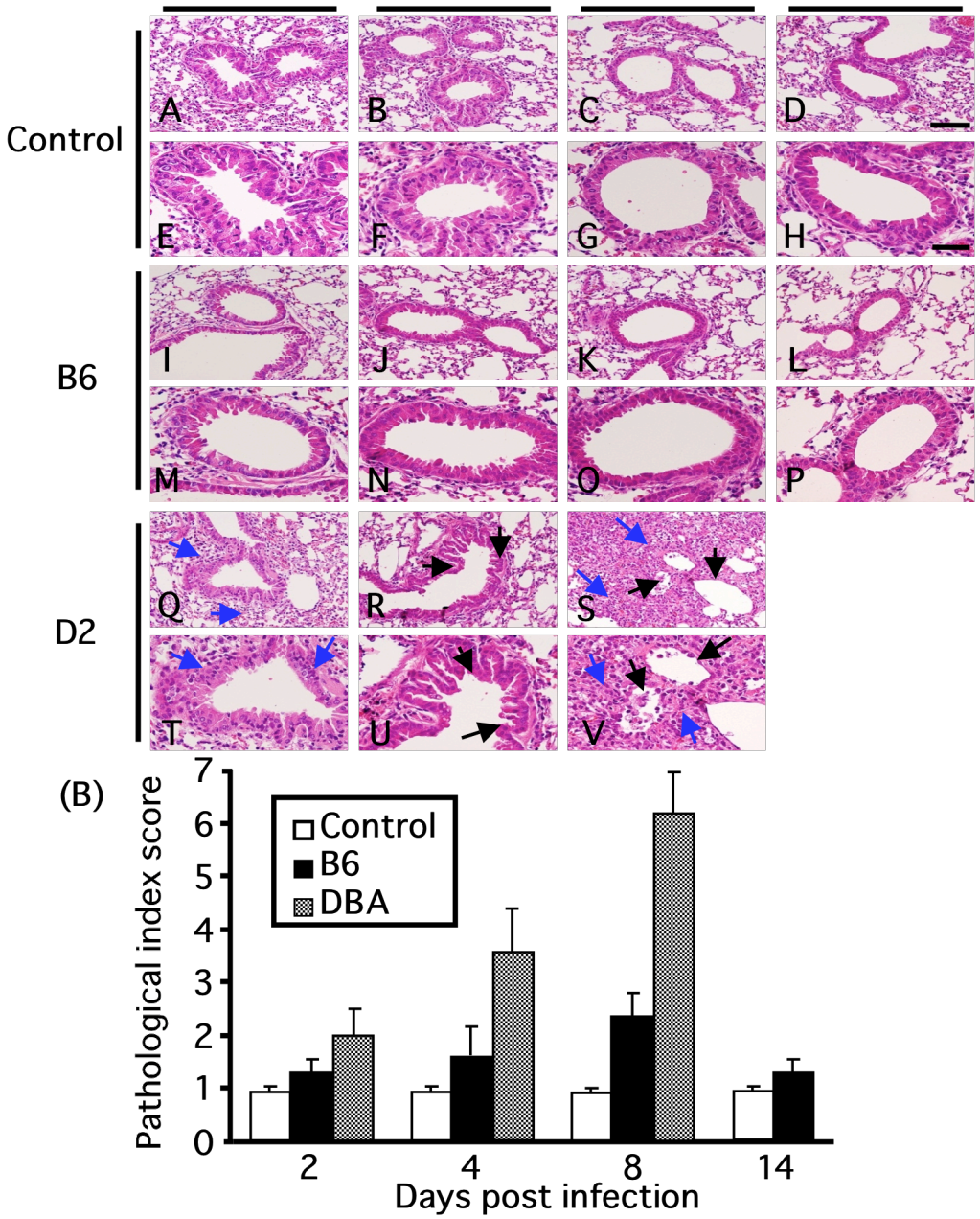

Fig 1.9. (A) Representative lung sections are shown for Control (panel A - H), B6 (panel I - P), and D2 mice (panel Q - V) for both lower (×20) and higher (×40) magnification. D2 mice had exudates in the alveolar spaces, this contain mixtures of cell debris epithelial cells, neutrophils, lymphocytes and morphologically altered macrophages (blue arrows), from day 4 to 8 p.i (panel R-V) the epithelial lining exhibited large areas of deciliation alternating with degeneration, necrosis, desquamation and marked hyperplasia with uneven thickness and cell arrangements (black arrows). B6 (panel I - P), on day 2 p.i the airways never contain exudates and their epithelium appeared generally intact, with the lamina propria containing a few noncoalescent foci of infiltration by mononucleated and lymphoid cells. All alveolar spaces were empty, with the exception of few macrophages neutrophils and lymphoid cells, the density of which was comparable to that observable in normal control lung. On day 4 and 8 p.i the interstitium, cell density appeared slightly elevated; however, this returned to normal by day 14. (B) Histogram illustrating the hematoxylin and eosin stain pathological index at indicated time points. Results are expressed as the mean values of the pathological index in the experimental groups. Error bars, 1 SE. Lung sections were stained with hematoxylin and eosin for histological evaluation, Bar = 50 μ m and 100 μ m.

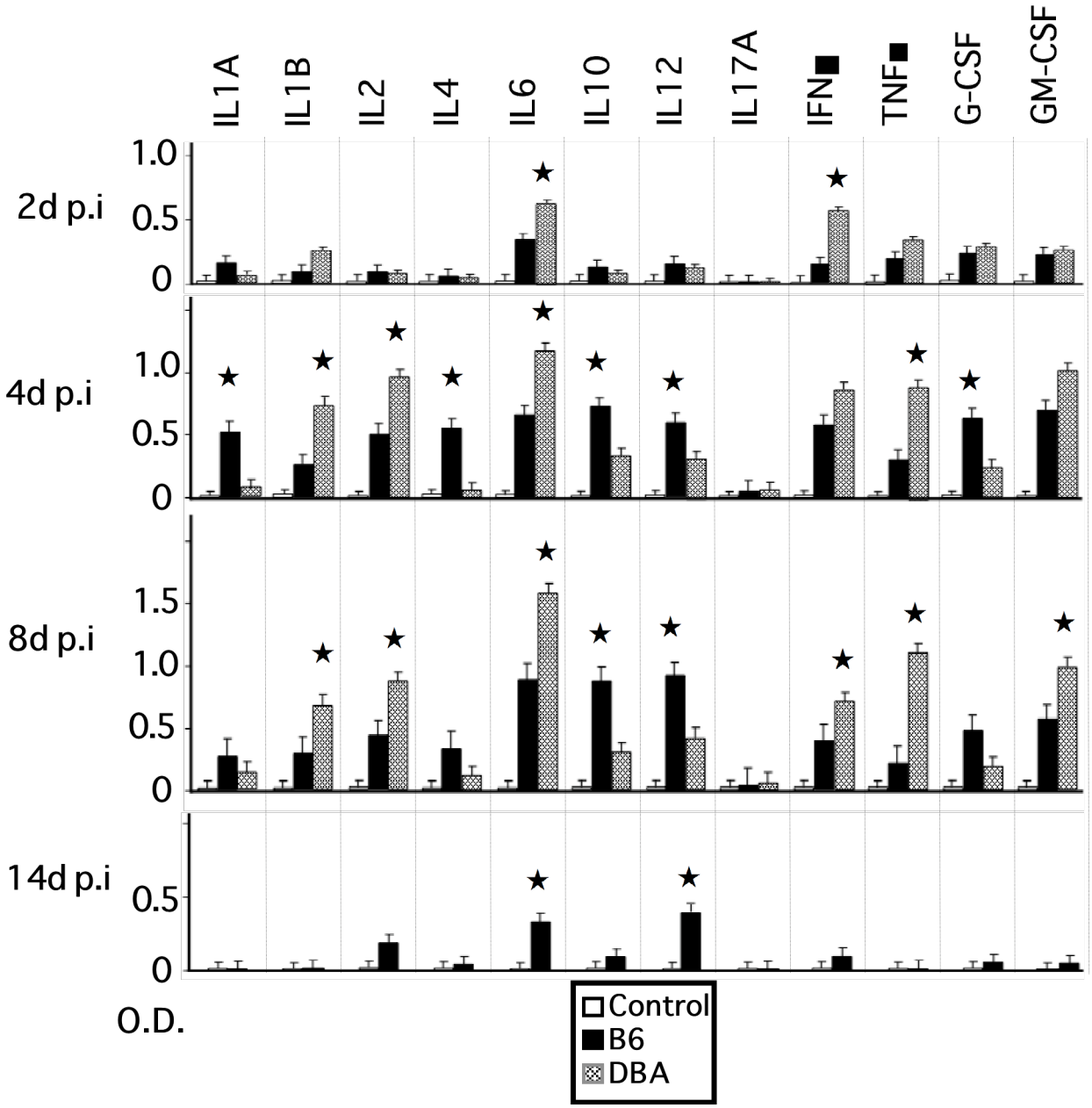

Fig 2.0. Pulmonary cytokine levels in bronchoalveolar lavage fluid of B6 (black bars), D2 (grey bars) and control (open bars) mice (n = 4 per group) following inoculation with SeV. BALF samples were collected on day 2, 4, 8 and 14, and cytokine levels were determined in duplicates using the mouse panel of Multi-Analyte ELISArray profiler. Data are expressed as mean± SEM of 4 mice at each time point. The detection limits of the assays were 2.5 OD at 450nm. Student t-test was used to determined the statistical differences between B6 and D2 mice, ★$P < 0.05$ B6 vs D2 on days 2, 4, and 8 or B6 vs control on day 14.

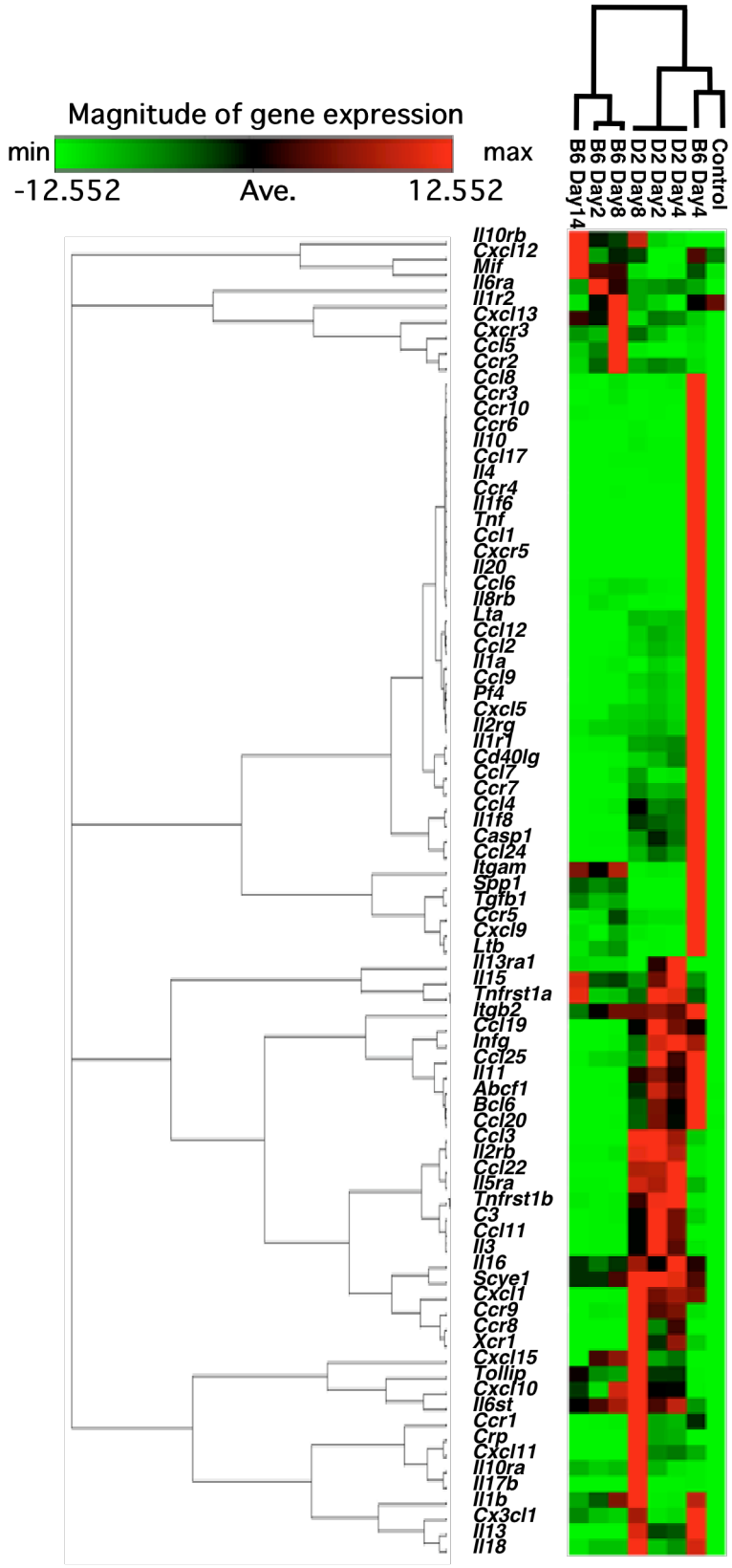

Fig 2.1. Cluster analysis showing heat map of mouse inflammatory cytokine/chemokine and receptor genes regulated in lungs of B6, D2 and control mice. A 2D gene tree was created using the average linkage clustering heat map method. Genes with a change in fold ($P < 0.001$) are depicted. Each row represents lung of each mouse group at indicated time points and the hierarchical structure of the time-points and infections is illustrated as a dendrogram while the fold change values are color encoded with green for down-regulated genes, black for average unregulated genes and red for up-regulated genes.

Table 1.5. Primer sequence of selected genes for quantitative-PCR

Gene	Primer sequence
Il11	5'-GGTGGTGCTGAGCCTCTGGC-3' (forward) 5'-GGCCCAGGGGGATCACAGGT-3' (reverse)
Il17b	5'-CTGCCGCCTGACTTGGTGGG-3' (forward) 5'-GTTGAGGACAGAGGCGGCGG-3' (reverse)
Spp1	5'-GCGGCAGGCATTCTCGGAGG-3' (forward) 5'-CGGCCGTTGGGGACATCGAC-3' (reverse)
Tgfb1	5'-GAAGCAGTGCCCGAACCCCC-3' (forward) 5'-CTCCGGTGCCGTGAGCTGTG-3' (reverse)
β-actin.	5'-TGTTACCAACTGGGACGACA-3' (forward) 5'- GGGGTGTTGAAGGTCTCAAA -3' (reverse)
SeV	5'-TCTGTTGAAGGCTGTCATGC-3' (forward) 5'-GAATGGGTTATCCGGGAGTT-3'(reverse)

Table 1.6. Log2 fold-changes in genes expression of inflammatory cytokines/chemokines and receptors in D2 susceptible compared to B6 resistant strain.

Accession No.	Gene Symbol	Gene Description	Up or Down	*P*-value
Chemokine gene				
NM_011329	*Ccl1*	Chemokine (C-C motif) ligand 1	2.18	0.638
NM_011330	***Ccl11***	Chemokine (C-C motif) ligand 11	7.3	0.000*
NM_011331	*Ccl12*	Chemokine (C-C motif) ligand 12	5.97	0.122
NM_011332	*Ccl17*	Chemokine (C-C motif) ligand 17	2.07	0.577
NM_011888	***Ccl19***	Chemokine (C-C motif) ligand 19	6.62	0.026*
NM_011333	*Ccl2*	Chemokine (C-C motif) ligand 2	4.02	0.186
NM_016960	***Ccl20***	Chemokine (C-C motif) ligand 20	6.62	0.052*
NM_009137	***Ccl22***	Chemokine (C-C motif) ligand 22	8.54	0.003*
NM_019577	*Ccl24*	Chemokine (C-C motif) ligand 24	7.25	0.093
NM_009138	*Ccl25*	Chemokine (C-C motif) ligand 25	3.52	0.093
NM_011337	***Ccl3***	Chemokine (C-C motif) ligand 3	9.01	0.005*
NM_013652	*Ccl4*	Chemokine (C-C motif) ligand 4	4.06	0.098
NM_013653	***Ccl5***	Chemokine (C-C motif) ligand 5	-3.52	0.003*
NM_013654	*Ccl7*	Chemokine (C-C motif) ligand 7	2.83	0.253
NM_011338	***Ccl9***	Chemokine (C-C motif) ligand 9	2.91	0.035*
NM_008176	***Cxcl1***	Chemokine (C-X-C motif) ligand 1	6.45	0.038*
NM_021274	***Cxcl10***	Chemokine (C-X-C motif) ligand 10	3.12	0.027*
NM_019494	*Cxcl11*	Chemokine (C-X-C motif) ligand 11	7.89	0.224
NM_011339	*Cxcl15*	Chemokine (C-X-C motif) ligand 15	6.58	0.29
NM_019932	*Cxcl4*	Chemokine (C-X-C motif) ligand 4	2.24	0.333
NM_009141	*Cxcl5*	Chemokine (C-X-C motif) ligand 5	2.09	0.089
Chemokine Receptors Genes				
NM_009912	*Ccr1*	Chemokine (C-C motif) receptor 1	4.69	0.061
NM_009835	*Ccr6*	Chemokine (C-C motif) receptor 6	2.33	0.549
NM_007719	*Ccr7*	Chemokine (C-C motif) receptor 7	6.31	0.132
NM_007720	***Ccr8***	Chemokine (C-C motif) receptor 8	10.23	0.001*
NM_009913	***Ccr9***	Chemokine (C-C motif) receptor 9	6.76	0.005*
NM_011798	***Xcr1***	Chemokine (C motif) receptor 1	8.33	0.004*
Cytokine Genes				
NM_008337	***Ifng***	Interferon gamma	6.59	0.050*
NM_008350	***Il11***	Interleukin 11	4.26	0.050*
NM_008355	*Il13*	Interleukin 13	8.89	0.077
NM_010551	***Il16***	Interleukin 16	7.38	0.004*
NM_019508	***Il17b***	Interleukin 17b	2.58	0.050*
NM_008360	*Il18*	Interleukin 18	2.23	0.19
NM_130058	*Il1f8*	Interleukin 1 family member 8	8.31	0.1
NM_010556	***Il3***	Interleukin 3	2.83	0.003*
NM_010735	*Lta*	Lymphotoxin A	7.34	0.126
NM_007926	***Scye1***	Small inducible cytokine subfamilyE, member 1	2.58	0.005*
NM_011616	*Cd40lg*	CD40 ligand	3.83	0.151
NM_008401	***Itgam***	Intergrin alpha M	-3.48	0.002*
NM_008518	***Ltb***	Lymphotoxin B	-3.51	0.005*
NM_009263	***Spp1***	Secreted phosphoprotein 1	-7.06	0.000*
NM_011577	***Tgfb1***	Transforming growth factor, beta 1	-5.78	0.003*
Cytokine Receptors Genes				
NM_008348	*Il10ra*	Interleukin 10 receptor, alpha	2.26	0.079
NM_133990	*Il13ra1*	Interleukin 13 receptor, alpha 1	2.58	0.33
NM_008362	*Il1r1*	Interleukin 1 receptor, type 1	3.06	0.131
NM_008368	***Il2rb***	Interleukin 2 receptor, beta chain	6.89	0.000*
NM_008370	***Il5ra***	Interleukin 5 receptor, alpha	6.62	0.004*
NM_010560	***Il6st***	Interleukin 6 signal transducer	2.87	0.005*
NM_011609	***Tnfrsf1a***	Tumor necrosis factor receptor subfamily, member 1a	2.62	0.016*
NM_011610	***Tnfrsf1b***	Tumor necrosis factor receptor subfamily, member 1b	6.15	0.000*
Other Genes Involved in inflammatory Response				
NM_013854	***Abcf1***	ATP-binding cassette, subfamily F member 1	5.23	0.053*
NM_009744	*Bcl6*	B-cell leukemia/lymphoma 6	6.28	0.06
NM_009778	***C3***	Complement component 3	6.18	0.004*
NM_009807	*Casp1*	Caspase 1	4.82	0.098
NM_007768	***Crp***	C-reactive protein, pentraxin-related	12.23	0.003*
NM_023764	***Tollip***	Toll interacting protein	3.23	0.034*

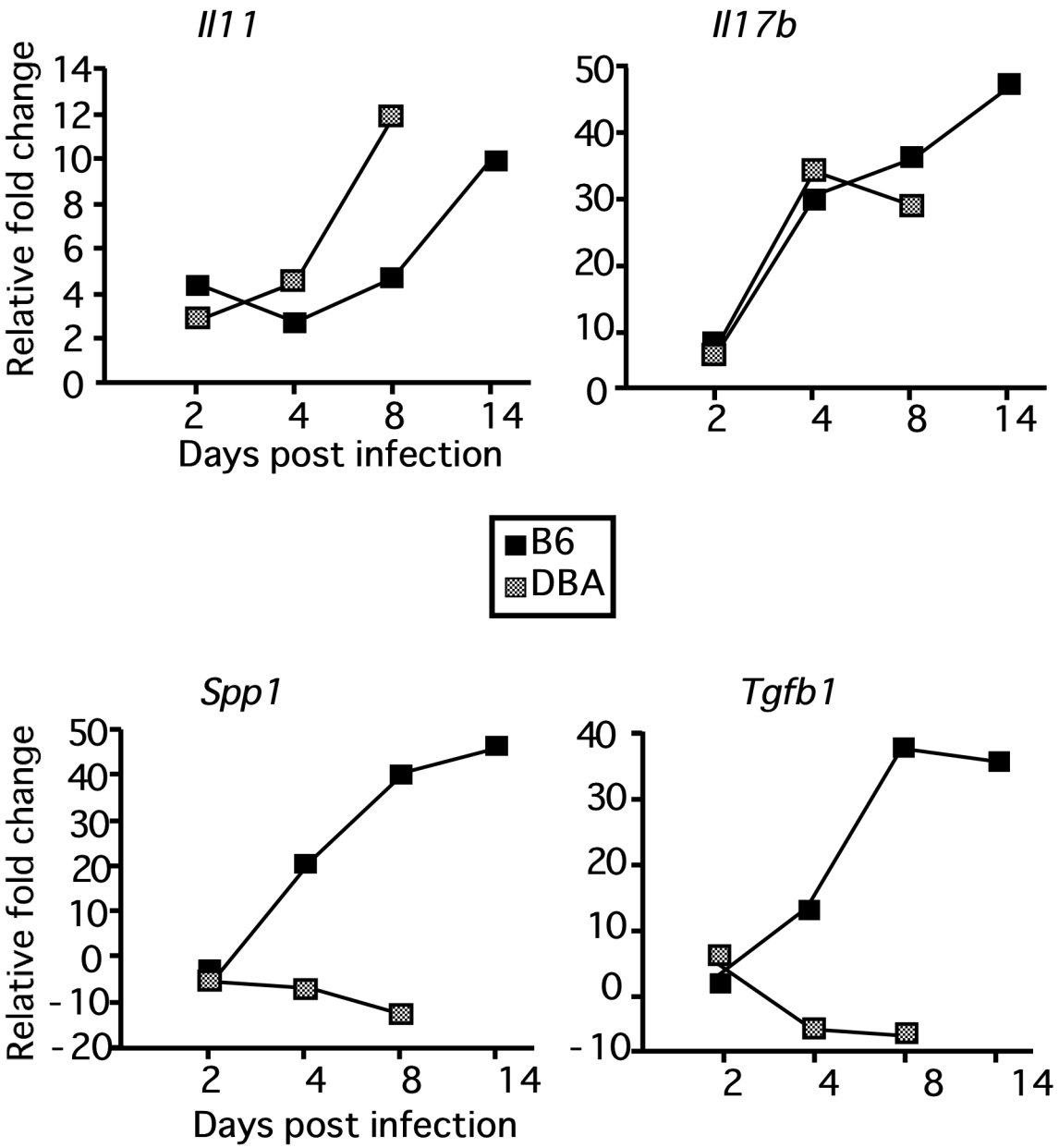

Fig 2.2. Validation of RT-PCR array by quantitative real time PCR; Data shows the relative gene expression through out the course of infection of up-regulated genes in both mice strains (A) *Il11*, (B) *Il17b* and down-regulated genes in D2 but up-regulated in B6 (C) *Spp1* and (D) *Tgfb1*.The house keeping gene *Actb* was used to normalize the expression of genes in all samples.

5.4 Discussion

The interface between an infectious agent and its host represents the ultimate battleground for survival: the microbe must secure a niche for replication, whereas the host must limit the pathogen's advance. Thus, following the initial observation that humans exhibit differential response to respiratory viruses and that certain mouse strains are more susceptible to SeV-induced pneumonia after infection, but other strains are resistant, the author sought to identify the underlying mechanism responsible for this strain difference. The data emphasize the overall complexity of the processes involved, because many differentially expressed gene products participate in anti-inflammatory regulatory circuits. Obviously, this reflects the enduring need for a local balance between effective immune protection and collateral damage.

At first sight (day 2 p.i), both strains seem to trigger a similar sequence of defensive events, which are typically characterized activation of tissue resident macrophages as well as recruitment of neutrophils. However, at later stages (day 4 and 8 p.i), signs of extensive cellular proliferation and tissue destruction, as well as T-cell-associated processes became apparent. These findings support the concept that both mice strains may elicit an innate immune response that is beneficial for virus control or on the other hand, may cause more extensive immunopathology. Susceptible D2 mice which succumbed to SeV infection had high viral loads and increased production of exuberant systemic proinflammatory cytokines/chemokines early after infection. In contrast, resistant B6 mice that effectively cleared the virus and produced lower levels of cytokines/chemokines. There was an intense pro-inflammatory and Th1 cytokine/chemokine response in D2 mice, which is associated with uncontrolled viral replication, which was very similar to the phenomena of acute influenza-infected

human patients and interestingly, the cytokine profile observed in this study, closely resembles that observed in highly pathogenic H5N1 influenza disease (de Jong et al., 2006). Similarly, H5N1 strongly induced production of CCL2, TNF-α, IFN-γ in susceptible D2 mice (Boon et al., 2009). Both previous reports are commonly associated with elevated plasma concentrations of IL-6, TNF-α, IFN-γ, CXCL10 (IP-10), CXCL9 (MIG) and CCL2 (MCP-1). In addition, the link between disease severity and high viral loads with increased production of proinflammatory cytokines was previously found in humans infected with Influenza and SARS viruses (Cameron et al., 2007).

SeV is an excellent inducer of IFN as well as other cytokines such as IL-2, TNF-α, IL-6 and IL-10, whose peaks were observed at the 7-10 day, about the time that the virus are cleared from the lungs (Mo et al., 1997a). However, there was distinct expression of some of these cellular proinflammatory mediators in BALF of these mice. For instance, the response in D2 mice was early and much more intense with the expression of high levels of IL-1ß, IL-2, IL-6, IFN-γ, TNF-α and GM-CSF, with low levels of IL-10 and IL-12, whereas B6 mice responded insidiously with moderate levels of IL-1α, IL-4, IL-10, IL-12, IFN-γ, G-CSF and GM-CSF. Cytokines/chemokines have the capacity to modulate and alter immune response of target cells. The balance of these bioactive molecules could determine the disease outcome for a susceptible animal. The virus-infected macrophages and dendritic cells, which reside in close proximity to epithelium, can produce significant amounts of IFNs and TNF-α and in response to SeV infection (Veckam et al., 2006). IFN-γ is one of the most important endogenous mediators of immunity and inflammation. IFN-γ plays a key role in macrophage activation, inflammation, host defense against intracellular pathogens and Th1 cell responses. In parallel, IFN-γ exerts regulatory functions to limit tissue damage associated with inflammation and to modulate

regulatory T cell differentiation. For instance, IFN-γ promotes innate immune responses by activating macrophages, enhances TLR induced production of TNF-α, IL-6 and IL-12. On the other hand, IFN-γ antagonizes anti-inflammatory effects of IL-10 both by attenuating IL-10 production, inhibition of TLR-induced *Il10* gene expression and by suppressing IL-10 signaling. At the same time, IFN-γ possesses crucial homeostatic functions that regulate the balance between clearance of invading pathogens and limiting collateral damage to the host (Hu and Ivashkiv, 2009). These results argue that D2 mice mount robust IFN-γ responses and exhibit high plasma levels of the IFN-stimulated cytokines TNF-α, IL-6 and lower amounts of IL-12, and together with CXCL10 and CCL2 chemokines during acute illness. Deregulation of IL-1ß, IL-6 and TNF-α production has been implicated in the pathology of several disease processes. Previous reports have shown that the temporal production of antiviral cytokine correlates with severity of viral illnesses (Cheung et al 2002, Szretter et al., 2007) and that IL-1ß, IL-6 and TNF-α are involved in inducing the severity of SeV infection and the lung immunopathology (Akk et al 2008), suggesting that the low amount of these cytokines protected B6 mice against the severity of SeV-induced excessive inflammation and weight loss. Th1 cells express high levels of IFN-γ, IL-2, and TNF-α, which activate macrophages to orchestrate a robust cell-mediated immune response. By comparison, Th2 cells express IL-4, IL-5, IL-10, and interact with B cells to generate strong humoral immune responses (Romagnani, 1995). The excess induction of IFN-γ by infectious pathogens has also been shown to play a role in the inhibition of the development of Th2 responses (Wohlleben and Erb, 2004). Consistently high levels of IFN-γ and IL-2, low levels of IL-4, IL-10 were detected in BALF of D2 mice, whereas, they were at higher levels in B6, suggesting that other migrating inflammatory cells in this strain are less efficient in the production of these mediators. This observation

suggested that Th1/Th2 polarization of the immune response following SeV infection determines susceptibility to the disease. Overall, primary SeV infection induces both Th1 and Th2 responses; however, there is a tendency for it to shift to Th1 as seen in susceptible D2 mice, while maintaining a balance in resistant B6 mice. Th1 cytokine IL-12, has been shown to reduce the severity of SeV-induced bronchiolar inflammation (Stone et al., 2003) and infected mice with any of these viruses; murine cytomegalovirus, respiratory syncytial virus, influenza virus and herpes simplex virus, increase in IL-12 levels are critical to early activation of NK cells and the establishment of a Th1 antiviral immune response (Romani et al., 1997). The effect of IL-12 on influenza virus immune response in resistant BALB/c mice showed that IL-12 contributes to the inhibition of early virus replication but is not required for virus clearance. In addition, IL-12 has been found to modestly contributes to the activation of cytotoxic T lymphocytes (Monteiro et al., 1998). These cytokines tend to form the bridge that trigger the activation of the adaptive immune response, confirming the lack of effective adaptive immune response in D2 mice hence the associated fatality observed in this strain. IL-4 also has been known to be produced during the course of this infection. This cytokine could be exerting a beneficial effects in B6 mice strain, since it has been shown to act synergistically with IL-12 in promoting T cell response (Mo et al., 1995). During acute influenza infection, $CD8^+$ T effector cells produce larger amount of IL-10, which controls excessive inflammation and associated tissue injury. In addition, blocking IL-10 resulted in enhanced pulmonary inflammation and lethal injury (Sun et al., 2009). In this study, B6 mice induced rapid and transient high level production of IL-10; in contrast, D2 mice produced low level of IL-10 during viral infection, suggesting the failure in regulation of the magnitude of inflammation during acute virus infection. The analysis also showed that quite a number of chemokine genes were

regulated upon SeV infection, indicating that the expression of chemokines is an important early host response during SeV infection and probably initiates cellular influx that were observed at later time points during the course of infection especially in D2 mice. This was similar to earlier studies of RSV infection of lung epithelial cells that resulted in a response dominated by chemokine expression and to others that analyzed chemokine expression in the lung (Zhang et al., 2001; Miller et al., 2004). Perhaps one of the most interesting findings was the set of genes that were consistently down-regulated in D2 mice while remaining up-regulated in B6 mice. For instance Ccl5 (RANTES) which had been known to interact with Ccr5 and provide antiapoptotic signals for macrophage survival during SeV infection and also accelerated recruitment of memory $CD8^+$ T cells to the lung airways during virus challenge thereby releasing effector molecules that impairs viral replication (Tyner et al., 2005; Kim et al., 2008), remained down-regulated in D2 mice. Possibly, this could account for the in ability of this strain to stop the cell-cell infectious process leading to delayed viral clearance and excessive airway inflammation, in contrast to B6 mice, that express both genes in a coordinated manner. In human blood dendritic-cell subsets, influenza virus triggers a coordinated secretion of several chemokines and chemokine receptors program in 3 successive waves with similar functions, thereby modulating the coordination of immune effectors in response to viral infection (Piqueras et al., 2006). For SeV infection, the severity of the disease might be linked to the extent of plasma leakage. For instance, several genes for cytokines/chemokines (IL-2, IL-6, TNF-α, INF-γ, GM-CSF, *Il18*, *Ccl2*, *Ccl3*, *Ccl5*, *Ccl7*, *Ccr2*, *Ccr3*) were also found to be up-regulated in D2 (Cheng and Chu, 2008). These gene products are known mediators of vascular permeability in addition to their regulatory functions of inflammatory responses. Therefore, the author postulated that, the upregulation of these cytokines and chemokines might be the

likely cause of severe hypoxemia in D2 mice. *Itgam*, *Tgfb1 Ltb* and *Spp1*, which have been known to play critical roles in inflammation; macrophage or T-cell activation and initiation of adaptive immune responses in response to viral infections (de Jong et al., 2006; Li and Flavell, 2008; Kim and Braciale, 2009) were also down-regulated in D2 mice. These data shows that, although D2 mice are able to mount immune responses early enough with the up-regulation of several cytokines and chemokines there exits a pathway in which these mice are deficient.

In conclusion, the important and novel finding of this study is that the deleterious immune inflammation seen in D2 mice is as a result of hypercytokinemia, or cytokine storm, during acute SeV pneumonia. In the previous crossing experiment involving these two strains described in Part 1, the author reported that, resistance was a dominant genetic trait under the control of three loci that encodes several genes. Similarly, the susceptibility seen in D2 mice might be under a similar genetic influence as seen with the upregulation of multiple cytokines and chemokines. However, the fact remains, that there are many genes involved in susceptibility and resistance to SeV, which can greatly influence the outcome of the disease. Thus, this comparative analysis of the pulmonary transcriptional signatures induced by SeV infection provides information on the molecular framework underlying pathogenesis and protective immunity in pneumonia. The identification of unique differences in gene expression profiles as well as common signatures can provide useful information for further molecular analysis and about suitable targets for novel intervention strategies, particularly with regard to the mechanisms responsible for the menacing similarities between respiratory viral infections. In addition, the two mice strains used in this study provides for models further elucidation respiratory viral immune responses to clearly define beneficial and detrimental responses in humans.

5.5 Summary

The severity of respiratory viral infections in humans varies in clinical presentations and pathological outcomes. To gain insight into the severity and differential immuno-pathogenesis of respiratory viral infections, Sendai virus (SeV) was used to define both beneficial and detrimental immune response in resistant C57BL6/J (B6) and susceptible DBA2/J (D2) mice. The kinetics of the differences in SeV-induced pneumonia and immune transcriptional signatures in lungs of these mice strains on days 2, 4, 8 and 14 after infection were compared. Cytokines in bronchoalveolar lavage fluid from lungs of these infected mice, were profiled and compared, and also the gene expressions of cytokines, chemokines and their receptors were also analyzed at indicated time points. The two mice strains were classically immunologically distinct, and D2 mice mounted an early and more intense immune response, with increased cellular influx which were dominated by macrophages, neutrophils and lymphocytes, high viral load, severe lung pathology and significant high levels of IL-1ß, IL-2, IL-6, IFN-γ, TNF-α and GM-CSF in contrast to B6 mice. Fifty six genes consistently showed an altered regulation in D2 mice, and of these numbers, 26 and 5 genes were significantly up-regulated and down-regulated, respectively, through out the course of infection as compared to B6 mice. These results suggest that the pronounced immune response observed in D2 mice might be instrumental to the severe pathology, thereby providing new insights into the pathogenesis of respiratory viral infections and highlighting the value of transcriptional profiling for the elucidation of underlying mechanisms.

7.0 General Conclusion

Sendai virus (SeV), also known as mouse parainfluenza virus type I, which is the archetype member of the paramyxovirus family that includes respiratory syncytial virus (RSV), human metapneumovirus, and human parainfluenza viruses that more often infect humans with high morbidity and mortality worldwide. The virus is used as a model to study human respiratory viral pathogenesis. In addition, it has been used extensively in studies that have defined most of the basic biochemical and molecular biologic properties of the paramyxoviruses. *In vivo* studies of most other paramyxoviruses are considerably more difficult because their susceptible hosts are often humans, non-human primates or other large animals and also because the mouse- or other small animal models do not always satisfactorily mimic natural infections and diseases. Hence the SeV-mouse system represents a good experimental paradigm for the dissection of host-viral interactions of respiratory viral infections. Different susceptibilities to SeV had been reported; however, there are no reports on the genetic basis for the varying response among mice strains. Thus, the author carried out a genetic mapping studies as well as trancriptome profiling to characterize the differential response in C57BL6/J (B6) and DBA2/J (D2) mice strains that represent two polar extremes in response to SeV infection.

The first part of the study involves genetic mapping studies in D2 susceptible and B6 resistant mice. F1, F2, and N2 backcrossed mice were generated and examined for their disease resistance and susceptibility. For the determination of virulence, percentage body weight loss and survival time were used as phenotypes. A genome wide scan on 108 backcrossed mice for linkage with percentage body weight loss as phenotype was performed. A major quantitative trait locus (QTL) showing significant linkage was mapped to the distal portion of Chr 4 (*SeV1*). In addition, two other QTLs showing

suggestive statistical linkage were also detected on Chr 8 and 14. Furthermore, genome scan was performed for interactions with least squares analysis of variance of all pairs of informative makers in backcrossed progenies. A highly significant epistatic interaction between *D3Mit182* and *D14Mit10* was identified, and denoted as *SeV2* and *SeV3*, respectively, and the latter was the same locus showing a suggestive level on Chr 14 in QTL analysis. Considered genotypes of these three loci, could account for more than 90% of genetic effect on the differential response to SeV infection between B6 and D2 mice. These findings revealed a novel gene interactions controlling SeV resistance in mice and will enable the identification of resistance genes encoded within these loci.

The second part of the study was perform to gain insight into the severity and differential immuno-pathogenesis of respiratory viral infections by defining both beneficial and detrimental immune response in resistant B6 and susceptible D2 mice. The author compared the differences in the kinetics of SeV-induced pneumonia and immune transcriptional signatures in lungs of these mice strains on days 2, 4, 8 and 14 after infection. Inflammatory cytokines in bronchoalveolar lavage fluid and gene expressions of cytokines, chemokines and their receptors from lungs of these infected mice were compared. The two strains were classically immunologically distinct, and D2 mice mounted an early and more intense immune response, with increased cellular influx which were dominated by macrophages, neutrophils and lymphocytes, high viral load, severe lung pathology and significant high levels of IL-1ß, IL-2, IL-6, IFN-γ, TNF-α and GM-CSF in contrast to B6 mice. Fifty six genes consistently showed an altered regulation in D2 mice, and of these numbers, 26 and 5 genes were significantly up-regulated and down-regulated, respectively, through out the course of infection as compared to B6 mice. These results suggest that the pronounced immune response observed in D2 mice

might be instrumental to the severe pathology and resembles “cytokine storm” of respiratory illness seen in humans.

Therefore, from these results the author conclude that, the important and novel finding of this study is that the deleterious immune inflammation observed in D2 mice results of hypercytokinemia, or cytokine storm, during acute SeV pneumonia. However, the fact remains, that there are many genes involved in susceptibility and resistance to SeV, which can greatly influence the outcome of the disease. Thus, the genetic mapping studies and comparative analysis of the pulmonary transcriptional signatures induced by SeV infection provides information on the molecular framework underlying pathogenesis and protective immunity in pneumonia. The identification of genetic loci that control resistance and unique differences in gene expression profiles as well as common signatures can provide useful information for further molecular analysis and about suitable targets for novel intervention strategies, particularly with regard to the mechanisms responsible for the menacing similarities between respiratory viral infections. Thus the two mice strains used in this study provides for models for further elucidation of respiratory viral immune responses to clearly define beneficial and detrimental responses in humans.

8.0 REFERENCES

1. Akk, A.M., Simmons, P.M., Chan, H.W., Agapov, E., Holtzman, M.J., Grayson, M.H., Pham, C.T. (2008). Dipeptidyl peptidase I-dependent neutrophil recruitment modulates the inflammatory response to sendai virus infection. J. Immunol. 180: 3535-3542.
2. Ali, A., Nayak, D.P. (2000). Assembly of Sendai virus: M protein interacts with F and HN proteins and with the cytoplasmic tail and transmembrane domain of F protein. Virology 276: 289-303.
3. Baig, E., Fish, E.N. (2008). Distinct signature type I interferon response are determined by the infecting virus and the target cell. Antivir. Ther. 13: 409-422.
4. Blanchard, L., Tarbouriech, N., Blackledge, M., Timmins, P., Burmeister, W.P., Ruigrok, R.W., Marion, D. (2004). Structure and dynamics of the nucleocapsid-binding domain of the Sendai virus phosphoprotein in solution. Virology 319: 201-211.
5. Blumberg, B.M., Giorgi, C., Rose, K., Kolakofsky, D. (1985). Sequence determination of the Sendai virus fusion protein gene. J. Gen. Virol 66: 317-331.
6. Boon, A.C., deBeauchamp, J., Hollmann, A., Luke, J., Kotb, M., Rowe, S., Finkelstein, D., Neale, G., Lu, L., Williams, R.W., Webby, R.J. (2009) .Host genetic variation affects resistance to infection with a highly pathogenic H5N1 influenza A virus in mice. J. Virol. 83:10417-26.
7. Bowman, M.C., Smallwood, S., Moyer, S.A. (1999). Dissect ion of individual functions of the Sendai virus phosphoprotein in transcription. J. Virol. 73: 6474-6483.
8. Breider, M.A., Adams, L.G., Womack, J.E. (1987). Influence of interferon in natural resistance of mice to Sendai virus pneumonia. Am. J. Vet. Res. 48: 1746-1750.
9. Broman, K.W., Wu, H., Sen, S. & Churchill, G.A. (2003). R/qtl: QTL mapping in experimental

crosses. Bioinformatics 19: 889-90.

10. Broman, K.W. (2003). Mapping quantitative trait Loci in the case of a spike in the phenotype distribution. Genetics 163: 1169-75.

11. Brownstein, D.G., Winkler, S. (1986). Genetic resistance to lethal Sendai virus pneumonia: virus replication and interferon production in C57BL/6J and DBA/2J mice. Lab. Anim. Sci. 36: 126-129.

12. Byers, D.E., Alevy, Y., Tucker, J., Swanson, S., Tidwell, R., Tyner, J.W., Morton, J.D., Castro, M., Polineni, D., Patterson, G.A., Schwendener, R.A., Allard, J.D., Peltz, G., Holtzman, M.J. (2008). Persistent activation of innate immune response translates respiratory viral infection into chronic lung disease. Nat. Med. 14: 633- 640.

13. Cai, X., Castleman, W.L. (2002). Increased IFN-gamma protein in bronchoalveolar lavage fluid of anti-IP-10 antibody-treated F344 rats following Sendai viral infection. J. Interferon Cytokine Res. 22:1175-9.

14. Cameron, M.J., Ran, L., Xu, L., Danesh, A., Bermejo-Martin, J.F., Cameron, C.M., Muller, M.P., Gold, W.L., Richardson, S.E., Poutanen, S.M., Willey, B.M., DeVries, M.E., Fang, Y., Seneviratne, C., Bosinger, S.E., Persad, D., Wilkinson, P., Greller, L.D., Somogyi, R., Humar, A., Keshavjee, S., Louie, M., Loeb, M.B., Brunton, J., McGeer, A.J. Canadian SARS Research Network, Kelvin DJ. (2007) Interferon-mediated immunopathological events are associated with atypical innate and adaptive immune responses in patients with severe acute respiratory syndrome. J. Virol. 81:8692-706.

15. Camp, N.J., Cox, A. (2002).Quantitative Trait loci: Methods and Protocols, Humana press, Totowa, New Jersey, USA.

16. Chanock, R.M., Murphy, B.R., Collins, P.L. (2001). Parainfluenza viruses. In: Fields, B.N., et al. (Eds.), Fields Virology. 4th ed. Lippincott Williams and Wilkins Philadelphia, PA, pp. 1341-1379.

17. Chen, J., Ng, M.M., Chu, J.J. (2008). Molecular profiling of T-helper immune genes during dengue virus infection. Virol. J. 5: 165

18. Chen, Y., Webster, R.G., Woodland, D.L. (1998). Induction of CD8+ T cell responses to dominant and subdominant epitopes and protective immunity to Sendai virus infection by DNA vaccination. J. Immunol. 160: 2425-2432.

19. Cheung, C.Y., Poon, L.L., Lau, A.S., Luk, W., Lau, Y.L, Shortridge, K.F., et al. (2002). Induction of proinflammatory cytokines in human macrophages by influenza A (H5N1) viruses: a mechanism for the unusual severity of human disease? Lancet. 360:1831-1837.

20. Cole, G.A., Katz, J.M., Hogg, T.L., Ryan, K.W., Porter, A.,Woodland, D.L. (1994). Analysis of the primary T-cell response to Sendai virus infection in C57BL/6 mice: CD4+Tcell recognition is directed predominantly to the hemmagglunin-neuraminidase glycoprotein. J. Virol. 68; 6863-6870.

21. Coronel, E.C., Murti, K.G., Takimoto, T., Portner, A. (2001). Nucleocapsid incorporation into parainfluenza virus is regulated by specific interaction with matrix protein. J. Virol. 75: 1117-1123.

22. Curran, J., Kolakofsky, D. (1988). Ribosomal initiation from an ACG codon in the Sendai virus P/C mRNA. EMBO J. 7: 245-251.

23. Curran, J., Kolakofsky, D. (1990). Sendai virus P gene produces multiple proteins from overlapping open reading frames. Enzyme 44: 244-249.

24. Curran, J., Marq, J.-B., Kolakofsky, D. (1995). An N-terminal domain of the Sendai paramyxovirus P protein acts as a chaperone for the NP protein during the nascent chain assembly step of genome

replication. J. Virol. 69: 849-855.

25. Das, S.C., Pattnaik, A.K. (2005). Role of the hypervariable hinge region of phosphoprotein P of vesicular stomatitis virus in viral RNA synthesis and assembly of infectious virus particles. J. Virol. 79: 8101-8112.

26. Darvasi, A. (1998). Experimental strategies for the genetic dissection of complex traits in animal models. Nat. Genet. 18: 19-24.

27. de Jong, M. D., Simmons, C. P., Thanh, T. T., Hien, V. M., Smith, G. J., Chau, T. N., Hoang, D. M., Chau, N. V., Khanh, T. H., Dong, V. C., Qui, P. T., Cam, B. V., Ha do, Q., Guan, Y., Peiris, J. S., Chinh, N. T., Hien, T. T., Farrar, J. (2006). Fatal outcome of human influenza A (H5N1) is associated with high viral load and hypercytokinemia. Nat. Med. 12:1203-1207.

28. Elco, C.P., Guenther, J.M., Williams, B.R., Sen, G.C. (2005). Analysis of genes induced by Sendai virus infection of mutant cell lines reveals essential role interferon regulatory factor 3, NF-kappaB, and interferon but not toll-like receptor 3. J. Virol. 79: 3920-3929.

29. Faisca, P., Bui Tran Anh, D., Desmecht, D. (2005). Sendai virus-induced alterations in lung structure/function correlate with viral loads and reveal a wide resistance/susceptibility spectrum among mouse strains. Am. J. Physiol. Lung Cell Mol. Physiol. 289: 777-787.

30. Faisca, P., Desmecht, D. (2007). Sendai virus, the mouse parainfluenza type-1: a long standing pathogen that remains up-to-date. Res. Vet. Sci. 82:115-125.

31. Fouillot-Coriou, N., Roux, L. (2000). Structure-function analysis of the Sendai virus F and HN cytoplasmic domain: different role for the two proteins in the production of virus particle. Virology 270: 464-475.

32. Frankel, W.N., Schork, N.J. (1996). Who's afraid of epistasis? Nat. Genet. 14: 371-373.

33. Fujii, Y., Sakaguchi, T., Kiyotani, K., Huang, C., Fukuhara, N., Egi, Y., Yoshida, T. (2002). Involvement of the leader sequence in Sendai virus pathogenesis revealed by recovery of a pathogenic field isolate from cDNA. J. Virol. 76: 8540-8547.

34. Garcin, D., Curran, J., Kolakosfky, D. (2000). Sendai virus C proteins must interact directly with cellular components to interfere with interferon action. J. Virol. 74: 8823-8830.

35. Gern, J.E., Brooks, G.D., Meyer, P., Chang, A., Shen, K., Evans, M.D., Tisler, C., Dasilva, D., Roberg, K.A., Mikus, L.D., Rosenthal, L.A., Kirk, C.J., Shult, P.A., Bhattacharya, A., Li, Z., Gangnon, R., Lemanske, R.F Jr. (2006). Bidirectional interactions between viral respiratory illnesses and cytokine responses in the first year of life. J. Allergy Clin. Immunol. 117:72-8.

36. Gotoh, B., Komatsu, T., Takeuchi, K., Yokoo, J. (2001). Paramyxovirus accessory proteins as interferon antagonists. Microbiol. Immunol. 45: 787-800.

37. Gotoh, B., Takeuchi, K., Komatsu, T., Yokoo, J. (2003). The STAT2 activation process is a crucial target of Sendai virus C protein for the blockade of alpha interferon signaling. J. Virol. 77: 3360-3370.

38. Grayson, M.H., Ramos, M.S., Rohlfing, M.M., Kitchens, R.,Wang, H.D., et al. (2007). Controls for lung dendritic cell maturation and migration during respiratory viral infection. J. Immunol. 179:1438-48.

39. Gupta, K.C., Patwardhan, S. (1988). ACG, the initiator codon for a Sendai virus protein. J. Biol. Chem. 263: 8553-8556.

40. Hausmann, S., Garcin, D., Delenda, C., and Kolakofsky, D. (1999). The versatility of paramyxovirus

RNA polymerase stuttering. J. Virol 73: 5568-5576.

41. Horikami, S.M., Hector, R.E., Smallwood, S., and Moyer, S.A. (1997). The Sendai virus Cprotein binds the L polymerase protein to inhibit viral RNA synthesis. Virology 235: 261-270.

42. Hou, S., Doherty, P.C., Zijlstra, M., Jaenisch, R., Katz, J.M. (1992). Delayed clearance of Sendai virus in mice lacking class I MCH restricted CD8+ T cells. J. Immunol. 149:1319-1325.

43. Itoh, M., Isegawa, Y., Hotta, H., and Homma, M. (1997). Isolation of an avirulent mutant of Sendai virus with two amino acid mutations from a highly virulent field strain through adaptation to LLC-MK2 cells. J. Gen. Virol. 78: 3207-3215.

44. Itoh, T., Saitoh, M., Iwai, H. (1989). Comparison of lung viral titers in susceptible and resistant inbred mouse strains against Sendai virus infection. Exp. Anim. 38: 269-273.

45. Itoh, T., Iwai, H., Ueda, K. (1991). Comparative lung pathology of inbred strains of mice resistant and susceptible to Sendai virus infection. J. Vet. Med. Sci. 53: 275-279.

46. Kast, W.M., Bronkhorst, A.M., De Wall, L.P., Melief, C.J. (1986). Cooperation between cytotoxic and helper T lymphocytes in protection against lethal Sendai virus infection. J. Exp. Med. 164: 723-738.

47. Kato, A., Kiyotani, K., Sakai, T., Yoshida, T., Nagai, Y. (1997). The paramyovirus, Sendai virus, V protein encodes a luxury function required for viral pathogenesis. EMBO J. 16, 578-587.

48. Kato, A., Cortese-Grogan, C., Moyer, S.A., Sugahara, F., Sakaguchi, T., Kubota, T., Otusuki, N., Kohase, M., Tashiro, M., Nagai, Y. (2004). Characterization of the amino acid residues of Sendai virus C protein that are critically involved in its interferon antagonism and RNA synthesis down-regulation. J. Virol. 78: 7443-7454.

49. Kato, H., Takeuchi, O., Sato, S., Yoneyama, M., Yamamoto, M.,Matsui, K., Uematsu, S., Jung, A., Kawai, T., Ishii, K.J., Yamaguchi, O., Otsu, K., Tsujimura, T., Koh, C.S., Reise, S.C., Matsuura, Y., Fujita, T., Akira, S. (2006). Differential roles of MDA5 and RIG-I helicases in the recognition of RNA viruses. Nature 441:101-105.

50. Kawai, T., and S. Akira. (2006). Innate immune recognition of viral infection. Nat. Immunol. 7:131-137..

51. Kim, T.S., Braciale, T.J. (2009). Respiratory dendritic cell subsets differ in their capacity to support the induction of virus-specific cytotoxic CD8+ T cell responses. PLoS One. 4: e4204.

52. Kim, E.Y., Battaile, J.T., Patel, A.C., You, Y., Agapov, E., Grayson, M.H., Benoit, L.A., Byers, D.E., Alevy, Y., Tucker, J., Swanson, S., Tidwell, R., Tyner, J.W., Morton, J.D., Castro, M., Polineni, D., Patterson, G.A., Schwendener, R.A., Allard, J.D., Peltz, G., Holtzman, M.J. (2008). Persistent activation of innate immune response translates respiratory viral infection into chronic lung disease. Nat. Med. 14: 633- 640.

53. Kingston, R.L., Hamel, D.J., Gay, L.S., Dahlquist, F.W., and Matthews, B.W. (2004). Structural basis for the attachment of a paramyxoviral polymerase to its template. Proc. Natl. Acad. Sci. 101: 8301-8306.

54. Kiyotani, K., Sakaguchi, T., Fujii, Y., and Yoshida, T. (2001). Attenuation of a field Sendai virus isolate through egg-passages is associated with an impediment of viral genome replication in mouse respiratory cells. Arch. Virol. 146: 893-908.

55. Kohlmeier, J.E., Miller, S.C., Smith, J., Lu, B., Gerard, C., Cookenham, T., Roberts, AD., Woodland, D.L. (2008). The chemokine receptor CCR5 plays a key role in the early memory CD8+ T cell response to respiratory virus infections. Immunity. 18:101-13.

56. Kurotani, A., Kiyotani, K., Kato, A., Shioda, T., Sakai, Y., Mizumoto, K., Yoshida, T., and Nagai, Y. (1998). Sendai virus C proteins are categorically nonessential gene products but silencing their expression severely impairs viral replication and pathogenesis. Genes Cells 3: 111-124.

57. Laham, F.R., Israele, V., Casellas, J.M., Garcia, A.M., Lac Prugent, C.M., Hoffman, S.J., Hauer, D., Thumar, B., Name, M.I., Pascual, A., Taratutto, N., Ishida, M.T., Balduzzi, M., Maccarone, M., Jackli, S., Passarino, R., Gaivironsky, R.A., Karron, R.A., Polack, N.R., Polack, F.P. (2004). Differential production of inflammatory cytokines in primary infection with human metapneumovirus and with other common respiratory viruses of infancy. J. Infect. Dis. 189: 2047-56.

58. Lamb, R.A., Kolakfsky, D. (2001). Paramyxoviridae: The viruses and their replication. In: Fields, B.N. et al. (Eds.), Fields Virology, fourth ed. Lippincott Williams & Wilkins, Philadelphia, PA, pp. 1305-1340.

59. Lander, E., Kruglyak, L. (1995). Genetic dissection of complex traits: guidelines for interpreting and reporting linkage results. Nat. Genet. 11: 241-7.

60. Latorre, P., Kolakofsky, D., Curran, J. (1998b). Sendai virus Y proteins are initiated by a ribosomal shunt. Mol. Cell. Biol. 18: 5021-5031.

61. Le Mercier, P., Garcin, D., Garcia, E., Kolakofsky, D. (2003). Competition between the Sendai virus N mRNA start site and the genome 3'-end promoter for viral RNA polymerase. J. Virol. 77: 9147-55.

62. Li, M.O., Flavell, R.A. (2008). Contextual regulation of inflammation: a duet by transforming growth factor-beta and interleukin-10. Immunity. 28: 468-76. Review

63. Lopez, C.B., Yount, J.S., Hermesh, T., Moran, T.M. (2006). Sendai virus infection induces adaptive immunity independently of type I interferons. J. Virol. 80: 4538-4545.

64. Manly, K.F., Cudmore Jr., R.H., Meer, J.M. (2001). Map Manager QTX, cross-plat form software for genetic mapping. Mamm. Genome. 12: 930-932.

65. Masters, P.S., Banerjee, A.K. (1988). Resolution of multiple complexes of phosphoprotein NS with nucleocapsid protein N of vesicular stomatitis virus. J. Virol. 62: 2651-2657.

66. Matikainen, S., Pirhonen, J., Miettinen, M., Lehtonen, A., Govenius-Vintola, C., Sareneva, T., Julkunen, I. (2000). Influenza A and Sendai viruses induce differential chemokine gene expression and transcription factor activation in human macrophages. Virology 276:138-147.

67. Medzhitov, R. (2001). Toll-like receptors and innate immunity. Nat. Rev. Immunol. 1:135-145.

68. Melendi, G.A., Laham, F.R, Monsalvo, A.C., Casellas, J.M, Israele, V., Polack, N.R., Kleeberger, S.R,, Polack, F.P. (2007). Cytokine profiles in the respiratory tract during primary infection with human metapneumovirus, respiratory syncytial virus, or influenza virus in infants. Pediatrics. 120: e410-5.

69. Miller, A. L., T. L. Bowlin., N. W. Lukacs. (2004). Respiratory syncytial virus-induced chemokine production: linking viral replication to chemokine production in vitro and in vivo. J. Infect. Dis. 189:1419-1430.

70. Miyamae, T. (2005). Differential invasion by Sendai virus of abdominal parenchymal organs and brain tissues in cortisone-and cyclophosphamide- based immunosupressed mice. J. Vet. Med. Sci.

67: 369-377.

71. Mo, X.Y., Sarawar, S.R., Doherty, P.C. (1995). Induction of cytokines in mice with parainfluenza pneumonia. J. Virol. 6: 1288-1291.

72. Mo, X.Y., Tripp, R.A., Sangster, M.Y., Doherty, P.C. (1997a). The cytotoxic T-lymphocyte response to Sendai virus is unimpaired in the absence of gamma interferon. J. Virol. 71:1906-10.

73. Mo, X.Y., Sangster, M.Y., Tripp, R.A., Doherty, P.C. (1997b). Modification of the Sendai virus-specific antibody and CD8+ T-cell responses in mice homozygous for disruption of the interleukin-4 gene. J. Virol. 71:2518-21.

74. Monteiro, J.M., Harvey, C., Trinchieri, G. (1998). Role of interleukin-12 in primary influenza virus infection. J. Virol. 72:4825-31.

75. Morgan, E.M., Rakestraw, K.M. (1986). Sequence of the Sendai virus L gene: open reading frames upstream of the main coding region suggest that the gene may be polycistronic. Virology 154: 31-40.

76. Morrison, T.G. (2003). Structure and function of a paramyxovirus fusion protein. Biochim. Biophys. Acta. 1614: 73-84.

77. Mottet, G., Mühlemann, A., Tapparel, C., Hoffmann, F., and Roux, L. (1996). A Sendai virus vector leading to the efficient expression of mutant M proteins interfering with virus particle budding. Virology 221: 159-171.

78. Ogino, T., Kobayashi, M., Iwama, M., Mizumoto, K. (2005). Sendai virus RNA-dependent RNA polymerase L protein catalyzes cap methylation of virus-specific mRNA. J. Biol. Chem. 280: 4429-4435.

79. Pennings, J.L, Kimman, T.G., Janssen, R. (2008). Identification of a common gene expression

response in different lung inflammatory diseases in rodents and macaques. PLoS One. 3: e2596.

80. Percy, D.H., Auger, D.C., Croy, B.A. (1994). Signs and lesions of experimental Sendai virus infection in two genetically distict strains of SCID/Beige mice. Vet. Pathol. 31: 67-73.

81. Piqueras, B., Connolly, J., Freitas, H., Palucka, A.K., Banchereau, J. (2006). Upon viral exposure, myeloid and plasmacytoid dendritic cells produce 3 waves of distinct chemokines to recruit immune effectors. Blood. 107:2613-8.

82. Poch, O., Blumberg, B.M., Bougueleret, L., and Tordo, N. (1990). Sequence comparison of five polymerases (L proteins) of unsegmented negative-strand RNA viruses: theoretical assignment of functional domains. J. Gen. Virol. 71: 1153-1162.

83. Qanungo, K.R., Shaji, D., Mathur, M., and Banerjee, A.K. (2004). Two RNA polymerase complexes from vesicular stomatitis virus-infected cells that carry out transcription and replication of genome RNA. Proc. Natl. Acad. Sci. 101: 5952-5957.

84. Rapp, J.P., Dene, H., Deng, A.Y., (1994). Seven rennin alleles in rats and their effects on blood pressure. J. Hypertens. 12: 349-355.

85. Romagnani, S. (1995). Biology of human Th1 and Th2 cells. J. Clin. Immunol. 15: 121-129.

86. Romani, L., Puccetti, P., Bistoni, F. (1997). Interleukin-12 in infectious diseases. Clin. Microbiol. Rev. 10:611-36.

87. Sakaguchi, T., Kiyotani, K., Sakaki, M., Fujii, Y., Yoshida, T. (1994a). A field isolate of Sendai virus: its high virulence to mice and genetic divergence form prototype strains. Arch. Virol. 135: 159-164.

88. Sakaguchi, T., Kiyotani, K., Sakaki, M., Fujii, Y., Yoshida, T. (1994b). A field isolate of Sendai

virus: its high virulence to mice and genetic divergence form prototype strains. Arch. Virol. 135, 159-164.

89. Sakaguchi, T., Kiyotani, K., Watanabe, H., Huang, C., Fukuhara, N., Fujii, Y., Shimazu, Y., Sugahara, F., Nazai, Y., Yoshida, T. (2003). Masking of the contribution of V protein to Sendai virus pathogenesis in an infection model with a highly virulent field isolate. Virology 13: 581-587.

90. Sanderson, C.M., McQueen, N.L., Nayak, D.P. (1993). Sendai virus assembly: M protein binds to viral glycoproteins in transit through the secretory pathway. J. Virol. 67: 651-663.

91. Shioda, T., Iwasaki, K., Shibuta, H. (1986). Determination of the complete nucleotide sequence of the Sendai virus genome RNA and the predicted amino acid sequences of the F, HN, and L proteins. Nucleic Acids Res. 14: 1545-1563.

92. Sidhu, M.S., Menonna, J.P., Cook, S.D., Dowling, P.C., Udem, S.A. (1993). Canine distemper virus L gene: sequence and comparison with related viruses. Virology 193: 50-65.

93. Skiadopoulos, M.H., Surman, S.R., Riggs, J.M., Elkins, W.R., St, C.M., Nishio, M., Garcin, D., Kolakofsky, D., Collins, P.L., and Murphy, B.R. (2002). Sendai virus, a murine parainfluenza virus type 1, replicates to a level similar to human PIV1 in the upper and lower respiratory tract of African green monkeys and chimpanzees. Virology 297: 153-160.

94. Smallwood, S., Moyer, S.A. (2004). The L polymerase protein of parainfluenza virus 3 forms an oligomer and can interact with the heterologous Sendai virus L, P and C proteins. Virology 318: 439-450.

95. Stone, A.E.S., Giguerre, S., Castleman, W.L. (2003). IL-12 reduces the severity of Sendai virus-induced bronchiolar inflammation and remodelling. Cytokine. 24: 103-113.

96. Strahle, L., Garcin, D., Le Mercier, P., Schlaak, J.F., Kolakofsky, D. (2003). Sendai virus targets inflammatory response, as well as the interferon-induced antiviral state, in a multifaceted manner. J. Virol. 77: 7903-7913.

97. Strahle, L., Marq, J.B., Brini, A., Huasmann, S., Kolakofsky, D., Garcin, D. (2007). Activation of the IFN beta promoter by natural Sendai virus infection requires RIG-I and is inhibited by viral C proteins. J. Virol. 81: 12285-12297.

98. Stricker, R., Mottet, G., Roux, L. (1994). The Sendai virus matrix protein appears to be recruited in the cytoplasm by the viral nucleocapsid to function in viral assembly and budding. J. Gen. Virol. 75: 1031-1042.

99. Sun, J., Madan, R., Karp, C.L., Braciale, T.J. (2009). Effector T cells control lung inflammation during acute influenza virus infection by producing IL-10. Nat. Med. 15:277-84.

100. Szretter, K.J., Gangappa, S., Lu, X., Smith, C., Shieh, W.J., Zaki, S.R, Sambhara, S., Tumpey, T.M., Katz, J.M. (2007). Role of host cytokine responses in the pathogenesis of avian H5N1 influenza viruses in mice. J. Virol. 81:2736-44.

101. Takimoto, T., Bousse, T., Coronel, E.C., Scroggs, R.A., Portner, A. (1998). Cytoplasmic domain of sendai virus HN protein contains a specific sequence required for its incorporation into virions. J. Virol. 72: 9747-9754.

102. Takimoto, T., Murti, K.G., Bousse, T., Scroggs, R.A., Portner, A. (2001). Role of matrix and fusion proteins in budding of Sendai virus. J. Virol 75: 11384-11391.

103. Tyner, J.W, Uchida, O., Kajiwara, N., Kim, E.Y., Patel, A.C., O'Sullivan, M.P., Walter, M.J., Schwendener, R.A., Cook, D.N., Danoff, T.M., Holtzman, M.J. (2005). CCL5-CCR5 interaction

provides antiapoptotic signals for macrophage survival during viral infection. Nat Med. 11:1180-7.

104. van der Sluijs, K.F., van Elden, L., Nijhuis, M., Schuurman, R., Florquin, S., Jansen, H.M., Lutter, R., van der Poll, T. (2003). Toll-like receptor 4 is not involved in host defence against respiratory tract infection with Sendai virus. Immunol. Lett. 89:201-206.

105. Veckman, V., Osterlund, P., Fagerlund, R., Melén, K., Matikainen, S., Julkunen, I. (2006). TNF-alpha and IFN-alpha enhance influenza-A-virus-induced chemokine gene expression in human A549 lung epithelial cells. Virology 345: 96-104.

106. Vidal, S., Curran, J., and Kolakofsky, D. (1992). Editing of the Sendai virus P/C mRNA by G insertion occurs during mRNA synthesis via a virus-encoded activity. J. Virol. 64: 239-246.

107. Wohlleben, G., Erb, KJ. (2004). The absence of IFN-gamma leads to increased Th2 responses after influenza A virus infection characterized by an increase in CD4+ but not CD8+ T cells producing IL-4 or IL-5 in the lung. Immunol Lett. 95: 161-6.

108. Yount, J.S., Gitlin, L., Moran, T.M., Lopez, C.B. (2008). MDA5 participates in the detection of paramyxovirus infection and is essential for the early activation of dendritic cells in response to Sendai virus defective interfering particles. J. Immunol. 180, 4910-4918.

109. Zhang, Y., B. A. Luxon, A. Casola, R. P. Garofalo, M. Jamaluddin, and A. R. Brasier. (2001). Expression of respiratory syncytial virus-induced chemokine gene networks in lower airway epithelial cells revealed by cDNA microarrays. J. Virol. 75: 9044-9058.

110. Zhong, W., Marshall, D., Coleclough, C., Woodland, D.L. (2000). CD4+ T cell priming accelerates the clearance of Sendai virus in mice, but has a negative effect on CD8+ T cell memory. J. Immunol. 164: 3274-3282.

111. Zhong, W., Roberts, A.D., Woodland, D.L. (2001). Antibody-independent antiviral function of memory CD4+ T cells in vivo requires regulatory signals from CD8+ effector T cells. J. Immunol. 167:1379- 1386.

112. Zondervan, K.T., Cardon, L.R. (2004). The complex interplay among factors that influence allelic association. Nat. Rev. Get. 5: 89-100.